A VISUALIZATION METHOD FOR BREAST CANCER DETECTION BY USING MICROWAVES

F. DELBARY*, M. BRIGNONE†, G. BOZZA‡, R. ARAMINI§, AND M. PIANA¶

Abstract. This paper proposes a qualitative approach to the inverse scattering problem of microwave tomography for breast cancer detection. In a 2D framework, the tumor inside the breast is regarded as an unknown scatterer placed inside an inhomogeneous and lossy background, formed by skin and fat. We firstly present in detail the mathematical formulation of the method, which is based on the reciprocity gap functional: in particular, the physical and geometrical properties of the healthy breast are coded into the Green's function of the corresponding scattering equation, while any other object outside the array of receiving antennas can be neglected. Then, we propose a "no-sampling" implementation of the method, which allows a very fast visualization of the breast slices (the computational time is around 1 s). Finally, we test the resulting algorithm against synthetic but realistic and noisy scattering data, by considering different plausible clinical situations.

Key words. Inverse scattering, microwave tomography, breast cancer detection, reciprocity gap functional.

1. Introduction. The gold standard for breast cancer detection is currently X-ray mammography, whereby images of a compressed breast are taken by using X-ray radiography. This technology can be used for both diagnostic purposes and screening plans aiming to detect cancer before the occurrence of any clinical sign. However, X-ray mammography presents significant drawbacks which are among the causes of the persistence of this disease. In particular, young age and high tissue density may result in false-positive or false-negative mammograms; the invasivity of X-ray ionizing radiation may limit the effectiveness of screening plans whose diffusion is also reduced by the cost of X-ray production. An interesting alternative for breast cancer detection could be using microwaves instead of X-rays [1]. Indeed microwaves assure a low degree of invasivity and an optimal contrast; furthermore, they can be produced by using cheap and easily available technologies. At microwave frequencies (from $3 \cdot 10^{-1}$ up to $3 \cdot 10^{1}$ GHz), the radiation-tissue interaction is defined by the electrical permittivity and the electrical conductivity of the tissue and therefore microwave imaging essentially means detecting inhomogeneities in the spatial distribution of these electrical parameters by using electromagnetic fields at microwave frequencies. More specifically, in tomographical frameworks [6, 23], a fixed-frequency microwave signal is transmitted from different positions and the diffracted field is collected by different antennas surrounding the breast, so that the inner part of the breast is imaged by reconstructing the spatial distribution of the electrical parameters.

From a mathematical viewpoint, microwave tomography can be formulated as a non-linear ill-posed inverse scattering problem [13] and several reconstruction methods have been proposed for its solution. For example, weak scattering approaches [15] linearize the non-linear inverse problem in the framework of Born-type approxi-

*Institut für Nümerische und Angewandte Mathematik, Universität Göttingen, 37083 Göttingen, Germany (delbary@math.uni-goettingen.de).

†CNR-INFM LAMIA, and Dipartimento di Matematica, Università di Genova, Via Dodecaneso 35, 16146 Genova, Italy (brignone@dima.unige.it).

‡Dipartimento di Bioingegneria Elettronica, Università di Genova (bozza@dibe.unige.it).

§Dipartimento di Ingegneria e Scienza dell'Informazione, Università di Trento, Via Sommarive 14, 38100 Povo di Trento, Italy (aramini@science.unitn.it).

¶CNR-INFM LAMIA, and Dipartimento di Matematica, Università di Genova, Via Dodecaneso 35, 16146 Genova, Italy (piana@dima.unige.it).

mations, thus allowing the applications of methods from the regularization theory for linear ill-posed problems [4]. However results from these procedures can be extremely inaccurate in the case of strong scattering effects, i.e. when the incident wavelengths are of the same size of the linear dimensions of the scatterer. A different approach consists in adopting non-linear optimization schemes [16], which are iterative techniques initialized by using a priori information on the electrical parameters and on the shape of the objects. These procedures can be very accurate but typically only if accurately initialized and, furthermore, they require heavy computational burdens.

In the last years several qualitative approaches to inverse scattering problems have been formulated [7], in which the presence and shape of inhomogeneities are visualized by solving sets of linear integral equations of the first kind. Qualitative approaches are faster than non-linear optimization, do not require a priori information on the scatterer to work, but are not able to provide pointwise estimates of the electrical parameters in the tissue (they only recover the set of points where these electrical parameters are different from a known background). In [10, 11] a qualitative approach, specifically the linear sampling method [12], is applied for visualizing leukemia in the bone marrow of the human leg. In the present paper, a qualitative method is formulated and applied for the detection of breast tumors in a two-dimensional microwave tomography framework. Our approach is a generalization of the method introduced in [8, 9], which, in turn, consists in matching the linear sampling method [7] with the reciprocity gap functional, in order to process near-fields instead of far-fields (as for traditional linear sampling). The generalization here consists in taking explicitly into account the heterogeneity of the background medium inside the array of receiving antennas. In other terms, the information on the healthy breast is encoded in the computation of the Green's function: in particular, since skin and fat are lossy media, this approach gives rise to an interior transmission problem involving complex wavenumbers, which deserves a careful discussion. Moreover, the implementation of the algorithm is realized by means of the "no-sampling" scheme [3, 5], already introduced for the linear sampling method, which allows an impressive rapidity in the visualization process (two-dimensional maps of the inner breast are obtained in around 1 s with a conventional PC).

2. The inverse scattering problem. The two-dimensional scattering problem modelling a microwave tomography experiment for breast cancer detection is described in Fig. 2.1. We consider an idealized geometrical model for the breast, whereby its axial view consists of a disk representing the fatty tissue, surrounded by a thin layer representing the skin. Embedded in the fat, the tumor takes up a spatial region assumed to be a bounded Lipschitz domain D such that the open complement of D is connected. In the space surrounding the breast, Γ and C denote two closed curves which are the boundaries of the bounded Lipschitz domains Ω and V respectively, with $\overline{\Omega} \subset V$. In the acquisition step, the receiving antennas will be placed on Γ and the emitting antennas will be placed on C. Since we work at a fixed (angular) frequency ω, in the following we shall not indicate the dependence on ω for the various physical quantities involved; we just recall that $\omega = k_0 c$, where k_0 and c are the wavenumber and the speed of light in free space respectively. We recall that the electrical properties of a generic medium are coded in the refractive index $\mathtt{n}(x)$, which is related to the electrical permittivity $\epsilon(x)$ and conductivity $\sigma(x)$ by the definition

$$\mathtt{n}(x) := \frac{1}{\epsilon_0}\left(\epsilon(x) + i\frac{\sigma(x)}{\omega}\right), \tag{2.1}$$

and to the wavenumber $\mathtt{k}(x)$ by the definition $\mathtt{k}^2(x) := k_0^2\mathtt{n}(x)$.

In this two-dimensional model of the breast, several different refractive indices and wavenumbers can be defined. First of all, in general, we will use the subscripts $0, 1, 2$ applied to electrical permittivity, electrical conductivity, refractive index and wavenumber to denote their constant value in free space (or coupling medium), fat, skin, respectively. In particular, we will assume $\sigma_0 = 0$ and $Im\{n_j\} > 0$ for $j = 1, 2$. Then $n_\Omega(x)$ and $k_\Omega(x)$ will denote the piecewise constant refractive index and wavenumber of the healthy medium contained in Ω (with $k_\Omega^2 = k_0^2 n_\Omega(x)$ for $x \in \Omega$). Outside Ω, the background $E := \mathbb{R}^2 \setminus \overline{\Omega}$ is formed by free space and several possible scatterers (e.g., walls, instrumentations) and is characterized by refractive index $n_E(x)$ and wavenumber $k_E(x)$. Therefore, in the case of a healthy breast, the refractive index and the wavenumber of the inhomogeneous medium in $\mathbb{R}^2$ are

$$n_b(x) := \begin{cases} n_\Omega(x) & x \in \Omega \\ n_E(x) & x \in E \end{cases} \quad \text{and} \quad k_b(x) := \begin{cases} k_\Omega(x) & x \in \Omega \\ k_E(x) & x \in E. \end{cases} \tag{2.2}$$

On the other hand, if a tumor D is present inside the fat, the refractive index and wavenumber of the medium in $\mathbb{R}^2$ are

$$\tilde{n}_b(x) := \begin{cases} n_D(x) & x \in D \\ n_b(x) & x \in \mathbb{R}^2 \setminus \overline{D} \end{cases} \quad \text{and} \quad \tilde{k}_b(x) := \begin{cases} k_D(x) & x \in D \\ k_b(x) & x \in \mathbb{R}^2 \setminus \overline{D}, \end{cases} \tag{2.3}$$

where $n_D(x)$ is the refractive index of the tumor and $k_D(x)$ is the corresponding wavenumber. Finally, for reasons related to the following computations, two auxiliary refractive indices and two auxiliary wavenumbers are introduced, i.e.:

$$n(x) := \begin{cases} n_\Omega(x) & x \in \Omega \\ 1 & x \in E \end{cases} \quad \text{and} \quad k(x) := \begin{cases} k_\Omega(x) & x \in \Omega \\ k_0 & x \in E, \end{cases} \tag{2.4}$$

and

$$\tilde{n}(x) := \begin{cases} n_D(x) & x \in D \\ n(x) & x \in \mathbb{R}^2 \setminus \overline{D} \end{cases} \quad \text{and} \quad \tilde{k}(x) := \begin{cases} k_D(x) & x \in D \\ k(x) & x \in \mathbb{R}^2 \setminus \overline{D}. \end{cases} \tag{2.5}$$

Accordingly to these different wavenumbers, for each $y \in \mathbb{R}^2$ different Green's functions can be defined. We denote with $G_b(\cdot, y)$ the Green's function for the equation describing the wave propagation in the entirely healthy background: in other terms, $G_b(\cdot, y)$ satisfies the equation $\Delta G_b(x, y) + k_b^2(x) G_b(x, y) = -\delta(x, y)$ in $\mathbb{R}^2$. Here $k_b(x)$ is assumed to be bounded everywhere and such that $k_b(x) = k_0$ for $|x| > R$ with R large enough. The Green's function corresponding to $k(x)$ is denoted by $G(\cdot, y) = G_y$ and, by superposition,

$$G_b(x, y) = G(x, y) + u_b^s(x, y) \quad \forall x, y \in \mathbb{R}^2, \quad x \neq y, \tag{2.6}$$

where $u_b^s(x, y)$ is the field scattered in x by the objects outside Ω when the pointlike source is located in y and only the media inside Ω are included in the background. As we shall see, one of the strengths of our visualization method is that the only Green's function we need to know in order to implement the algorithm is G_y. Some discussions about how to explicitly determine it will be given later in the text. Finally, $\tilde{G}_b(x, y)$ is the Green's function corresponding to $\tilde{k}_b(x)$. It is possible to show [18] that the following symmetry properties hold:

$$G(x, y) = G(y, x), \quad G_b(x, y) = G_b(y, x), \quad \tilde{G}_b(x, y) = \tilde{G}_b(y, x), \quad \forall x \neq y. \tag{2.7}$$

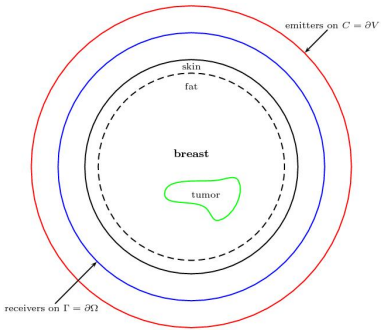

FIG. 2.1. *Scheme of the 2D microwave tomography experiment for breast cancer detection.*

Finally, we introduce the notations for some functional spaces we shall use in the next sections:

$$H^s_\Delta(D) := \{u \in H^s(D) \ : \ \Delta u \in L^2(D)\}, \quad \text{for } s = 0, 1; \tag{2.8}$$

$$K^s_1 := \{u \in H^s(D) \ : \ \Delta u + k_1^2 u = 0 \text{ in } D\}, \quad \text{for } s = 0, 1; \tag{2.9}$$

$$K^s_D := \{u \in H^s(D) \ : \ \Delta u + k_D^2(x) u = 0 \text{ in } D\}, \quad \text{for } s = 0, 1. \tag{2.10}$$

We can easily realize that the following inclusions hold for $s = 0, 1$: $K^1_1 \subset K^0_1$, $K^1_D \subset K^0_D$, $K^s_1 \subset H^s_\Delta(D)$, $K^s_D \subset H^s_\Delta(D)$. Furthermore, $H^s_\Delta(D)$, K^s_1 and K^s_D equipped with the norm defined as $\|u\|^2_{H^s_\Delta(D)} := \|u\|^2_{H^s(D)} + \|\Delta u\|^2_{L^2(D)}$, with $s = 0, 1$, are Hilbert spaces. It is easy to realize that for the spaces K^s_1 and K^s_D the $H^s_\Delta(D)$-norm is equivalent to the $H^s(D)$-norm. Finally, following the same approach as that of Theorem 4.2 in [24], it can be proved that K^1_1 is dense in K^0_1 with respect to the $L^2(D)$-norm.

3. The Reciprocity Gap Functional equation. Let us assume that $k_D \in L^\infty(D)$ and that there exists a positive real number c_D such that $\mathcal{I}m\{n_D(x)\} \geq c_D > 0$ for almost all (f.a.a.) $x \in D$. In the case of a TM-polarized time-harmonic incident wave $u^i = u^i(\cdot, x_0)$ chosen as the Green's function $G_b(\cdot, x_0)$ for $x_0 \in \mathbb{R}^2 \setminus \overline{D}$, the spatial part $u = u(\cdot, x_0)$ of the total electric field satisfies the forward problem [9]

$$\begin{cases} \Delta u + \tilde{k}_b^2(x) u = 0 \quad \text{in} \quad \mathbb{R}^2 \setminus \{x_0\} \\ u = u^s + u^i \\ \lim\limits_{r \to \infty} \sqrt{r}(\partial_r u^s - \mathrm{i} k_0 u^s) = 0, \end{cases} \tag{3.1}$$

where $\partial_r := \frac{\partial}{\partial r}$. Problem (3.1) can be equivalently expressed in integral form by means of the Lippmann-Schwinger equation: then, by following an approach analogous to that of chapter 8 in [13], it can be shown that, for each $x_0 \in \mathbb{R}^2 \setminus \overline{D}$, there exists a unique solution $u = u(\cdot, x_0) \in H^1_{loc}(\mathbb{R}^2 \setminus \{x_0\})$ of problem (3.1). We observe that this solution is the Green's function $G_b(\cdot, x_0)$: in particular, by virtue of (2.7), we have the reciprocity property $u(x, x_0) = u(x_0, x)$ for all $x_0 \in \mathbb{R}^2 \setminus \overline{D}$ and $x \in \mathbb{R}^2 \setminus \{x_0\}$.

The inverse scattering problem considered in this paper is that of inferring information on $\tilde{k}_b^2(x)$ and, in particular, on $n_D(x)$, from the knowledge of $u^s(x, x_0)$ at different (discretized) x-locations, for a suitable number of emitting antennas placed at different x_0-locations and sending the known fields $u^i(\cdot, x_0)$; of course, $u^s(x, x_0)$ is obtained from measurements of $u(x, x_0)$, by remembering that $u^s = u - u^i$. This

inverse problem is ill-posed in the sense of Hadamard [13] and, at microwave frequencies, it is highly non-linear. We will address this problem by means of a qualitative approach, which will be able to reconstruct the support $\overline{D}$ of the tumor without providing any information on the point values of $n_D(x)$.

For two functions u, v in $H^1_\Delta(\Omega)$, the Reciprocity Gap Functional (RGF) is defined as

$$\mathcal{R}(u,v) := \int_\Gamma \left[u(x)\partial_\nu v(x) - v(x)\partial_\nu u(x)\right] ds(x), \tag{3.2}$$

where $\partial_\nu := \frac{\partial}{\partial \nu}$, being ν the unit normal vector to $\Gamma = \partial\Omega$, directed into the exterior of Ω. The visualization method utilized for the microwave tomography application in this paper is based on the analysis of the family of RGF equations (parameterized over the sampling point $z \in \Omega$) [9]

$$\mathcal{R}(u(\cdot, x_0), s_g) = \mathcal{R}(u(\cdot, x_0), G_z) \quad \forall x_0 \in C, \tag{3.3}$$

where the unknown is a function $g \in H^{-1/2}(C)$, $G_z = G(\cdot, z)$, s_g is the single-layer potential of density g

$$s_g(x) := \int_C G(x,y)g(y)ds(y), \quad x \in \mathbb{R}^2 \setminus C, \tag{3.4}$$

and, as above, $u(\cdot, x_0)$ is the unique solution to problem (3.1) when the incident wave is sent by a point $x_0 \in C$; for future reference, we introduce the set U of all such solutions, i.e.: $U := \{u(\cdot, x_0) \ : \ x_0 \in C\}$.

In order to perform the analysis of the family of RGF equations (3.3), we need to introduce the following three operators:

$$F \ : \ H^{-\frac{1}{2}}(C) \to L^2(C), \quad g \overset{F}{\mapsto} \left[x_0 \mapsto \mathcal{R}(u(\cdot, x_0), s_g)\right], \tag{3.5}$$

$$H \ : \ H^{-\frac{1}{2}}(C) \to K_1^0, \quad g \overset{H}{\mapsto} s_g|_D, \tag{3.6}$$

$$P \ : \ K_1^0 \to L^2(C), \quad v \overset{P}{\mapsto} \left[x_0 \mapsto \int_D \left[k_1^2 - k_D^2(x)\right] v(x)u(x, x_0)dx\right]. \tag{3.7}$$

The aim of this section is to study some relevant properties of these operators, according to a plan consisting of the following main points:
Point 1: we show that F can be written as the product of $-P$ and H (Theorem 3.1);
Point 2: we prove that H is injective with dense range (Theorem 3.2);
Point 3: we prove that P is injective with dense range (Theorem 3.6), which, together with points 1 and 2, implies that F is injective with dense range (Corollary 3.7);
Point 4: we give an exact characterization of D via the range of P (Theorem 3.8);
Point 5: we prove the general theorem qualitatively characterizing D in terms of the behavior of approximate solutions to the family of RGF equations (Theorem 3.9): this theorem will inspire the visualization algorithm described in the next section.

We now discuss the five points in detail.

Point 1.

THEOREM 3.1. *The operator F is compact and can be factored as $F = -PH$.*

Proof. From definitions (3.2) and (3.5), it easily follows that F is an integral operator with regular kernel $S : C \times C \to \mathbb{C}$ defined as $S(x_0, y) := \mathcal{R}(u(\cdot, x_0), G(\cdot, y))$. In particular, the range of F is a subset of $H^1(C)$, which is compactly embedded in $L^2(C)$ [20]: this shows the compactness of F.

As regards the factorization $F = -PH$, for any $g \in H^{-\frac{1}{2}}(C)$ let us define $v \in H^1_\Delta(\Omega)$ as $v := s_g|_\Omega$. Then, from (3.4) and (3.5), we get $Fg(x_0) = \mathcal{R}(u(\cdot, x_0), s_g) = \mathcal{R}(u(\cdot, x_0), v)\ \forall x_0 \in C$, so that, remembering definition (3.2),

$$Fg(x_0) = \int_\Gamma u(x, x_0)\partial_\nu v(x) ds(x) - \int_\Gamma v(x)\partial_{\nu_x} u(x, x_0) ds(x) \quad \forall x_0 \in C. \tag{3.8}$$

Since both $u(\cdot, x_0)|_\Omega, v \in H^1_\Delta(\Omega)$ satisfy in $\Omega \setminus \overline{D}$ the equation

$$\Delta u + k^2(x)u = 0, \tag{3.9}$$

applying the second Green's identity in $\Omega \setminus \overline{D}$ to the right-hand side of (3.8) gives:

$$Fg(x_0) = \int_{\partial D} u(x, x_0)\partial_\nu v(x) ds(x) - \int_{\partial D} v(x)\partial_{\nu_x} u(x, x_0) ds(x) \quad \forall x_0 \in C. \tag{3.10}$$

Then, if we observe that $u(\cdot, x_0)|_D \in K^1_D$ and $v|_D \in K^1_1$, we can still apply the second Green's identity in D and rewrite equality (3.10) as:

$$Fg(x_0) = -\int_D \left[k_1^2 - k_D^2(x)\right] u(x, x_0)v(x) dx \quad \forall x_0 \in C, \tag{3.11}$$

i.e., by definitions (3.6) (in particular, $v|_D = Hg$) and (3.7), $Fg(x_0) = -PHg(x_0)$ $\forall x_0 \in C$. This concludes the proof. □

Point 2.

THEOREM 3.2. *The operator H is injective and has a dense range with respect to the $L^2(D)$-norm.*

Proof. We split the proof into three steps.

Step 1: H is injective. Suppose that $g \in H^{-\frac{1}{2}}(C)$ is such that $Hg = 0$. Then, remembering definition (3.6), we have that $s_g = 0$ in D. Moreover, since $s_g \in H^1(V)$ verifies equation (3.9) in V, we have $s_g = 0$ in V by virtue of the unique continuation principle [19]. Hence, also the trace on $C = \partial V$ of s_g is zero, i.e. $S_C g = 0$, where $S_C : H^{-1/2}(C) \to H^{1/2}(C)$ such that $g \mapsto S_C g := s_g|_C$ is the single-layer operator on C [20]. Since, as stated before, we assume that $\mathcal{I}m\{n_j\} > 0$ for $j = 1, 2$, it is possible to prove (see Theorem A.2 in Appendix A) that S_C is injective. Then, $S_C g = 0$ implies $g = 0$.

Step 2: $\tilde{H}$ has a dense range. Let us define the operator $\tilde{H} : H^{-\frac{1}{2}}(C) \to H^{\frac{1}{2}}(\partial D)$, with $\tilde{H}(g) := s_g|_{\partial D}$, and prove that it has a dense range: this amounts to proving that the transpose operator ${}^t\tilde{H} : H^{-\frac{1}{2}}(\partial D) \to H^{\frac{1}{2}}(C)$, with ${}^t\tilde{H}(f) = \int_{\partial D} G(x, y)f(y)ds(y)$, is injective. We note that for all $f \in H^{-\frac{1}{2}}(D)$, ${}^t\tilde{H}f$ is the trace on C of the single-layer potential of density f on ∂D (cf. definition (3.4)). Now, let us suppose that $f \in H^{-\frac{1}{2}}(\partial D)$ is such that ${}^t\tilde{H}f = 0$: we want to prove that $f = 0$. To this end, let us consider the single-layer potential v of density f on ∂D, i.e. $v(x) := \int_{\partial D} G(x, y)f(y)ds(y)$ for $x \in \mathbb{R}^2 \setminus \partial D$. Of course, v is a radiative solution of equation (3.9) in $\mathbb{R}^2 \setminus \overline{D}$. Moreover, the assumption ${}^t\tilde{H}f = 0$ means that v vanishes identically on $C = \partial V$: hence, by virtue of Theorem A.1 in Appendix A, we have $v = 0$ in $\mathbb{R}^2 \setminus \overline{V}$ and then the unique continuation principle ensures that $v = 0$ in $\mathbb{R}^2 \setminus \overline{D}$. As a consequence, we get $S_{\partial D} f = 0$, where $S_{\partial D} : H^{-1/2}(\partial D) \to H^{1/2}(\partial D)$ is the single-layer operator on ∂D. Analogously to the end of the previous Step 1, we can now conclude that $f = 0$ by using the injectivity of $S_{\partial D}$.

Step 3: H has a dense range. We want to show that for any $w \in K_1^0$ and $\epsilon > 0$, there exists $g \in H^{-1/2}(C)$ such that

$$||Hg - w||_{L^2(D)} < \epsilon. \tag{3.12}$$

To this end, we firstly recall that K_1^1 is dense in K_1^0 with respect to the $L^2(D)$-norm: hence, there exists $v \in K_1^1$ such that

$$||v - w||_{L^2(D)} < \frac{\epsilon}{2}. \tag{3.13}$$

Then, we observe that the continuous dependence of the solution of a strongly elliptic equation on the boundary data [20] implies the existence of a constant $\alpha > 0$ such that for all $\psi \in K_1^1$ it holds

$$\|\psi\|_{H^1(D)} \leq \alpha \|\psi|_{\partial D}\|_{H^{\frac{1}{2}}(\partial D)}. \tag{3.14}$$

Now, remembering the previous Step No. 2, we can choose $g \in H^{-\frac{1}{2}}(C)$ such that

$$\left\|\tilde{H}g - v|_{\partial D}\right\|_{H^{\frac{1}{2}}(\partial D)} < \frac{\epsilon}{2\alpha}. \tag{3.15}$$

Moreover, since both $Hg = s_g|_D \in H^1(D)$ and $v \in K_1^1$ (and consequently $Hg - v$) solve equation $\Delta\psi + k_1^2\psi = 0$ in D, by virtue of inequalities (3.14) and (3.15) we have

$$\|Hg - v\|_{H^1(D)} \leq \alpha \|(Hg - v)|_{\partial D}\|_{H^{\frac{1}{2}}(\partial D)} = \alpha \left\|\tilde{H}g - v|_{\partial D}\right\|_{H^{\frac{1}{2}}(\partial D)} < \frac{\epsilon}{2}. \tag{3.16}$$

Hence, by using the triangle inequality together with relations (3.13), (3.16) and remembering that the $L^2(D)$-norm is bounded by the $H^1(D)$-norm, we obtain relation (3.12), which concludes the proof. □

Point 3.

In order to establish the main result of this point 3, i.e. Theorem 3.6, we firstly need to prove the following three lemmas.

LEMMA 3.3. *The set $U_D = \{u|_D : u \in U\}$ is dense in K_D^1 with respect to the $L^2(D)$-norm.*

Proof. Let $v \in U_D^{\perp}$: this means that $v \in K_D^1$ is such that $(u, v)_{L^2(D)} = 0$ for all $u \in U_D$, i.e.

$$\int_D u(x, x_0)\bar{v}(x)dx = 0 \quad \forall x_0 \in C. \tag{3.17}$$

As already observed, for all $x_0 \in \mathbb{R}^2 \setminus \overline{D}$, in $\mathbb{R}^2 \setminus \{x_0\}$ it holds $u(\cdot, x_0) = \tilde{G}_b(\cdot, x_0)$, where $\tilde{G}_b(\cdot, x_0)$ is the Green's function for the first equation in problem (3.1), which takes into account the presence of the tumor. Now, let us define

$$w(x) := \int_D \tilde{G}_b(y, x)\bar{v}(y)dy \quad \forall x \in \mathbb{R}^2. \tag{3.18}$$

In particular, by virtue of the previous observation, we have $w(x) = \int_D u(y, x)\bar{v}(y)dy$ $\forall x \in \mathbb{R}^2 \setminus \overline{D}$ and, as a consequence of (3.17), $w(x_0) = 0$ $\forall x_0 \in C$. Moreover, $w = w(x)$ is clearly a radiative solution of $\Delta w + \tilde{k}_b^2(x)w = 0$ in $\mathbb{R}^2 \setminus \overline{D}$ and, as just stated, it vanishes on $C = \partial V$; hence, by applying Theorem A.1 in Appendix

A, we have $w = 0$ in $\mathbb{R}^2 \setminus V$ and, by virtue of the unique continuation principle, $w = 0$ in $\mathbb{R}^2 \setminus \overline{D}$: in particular, it holds $w|_{\partial D} = 0$, $\partial_\nu w|_{\partial D} = 0$. Moreover, as a direct consequence of definition (3.18), w verifies $\Delta w + \tilde{k}_b^2(x)w = -\bar{v}$ in D, whence $\int_D (\Delta w)(x)v(x)dx + \int_D \tilde{k}_b^2(x)w(x)v(x)dx = -\|v\|^2_{L^2(D)}$, i.e., by virtue of the second Green's identity [20] and remembering that $w|_{\partial D} = 0$, $\partial_\nu w|_{\partial D} = 0$,

$$\int_D \left[\Delta v(x) + \tilde{k}_b^2(x)v(x)\right] w(x)dx = -\|v\|^2_{L^2(D)}. \tag{3.19}$$

But $v \in K_D^1$, then, by virtue of definitions (2.2) and (2.10), the left-hand side of (3.19) is zero: hence we have $\|v\|^2_{L^2(D)} = 0$, i.e. $v = 0$. This concludes the proof. □

LEMMA 3.4. *The following operator:*

$$M \ : \ H^{\frac{1}{2}}(\partial D) \to L^2(C), \quad v \overset{M}{\mapsto} \left[x_0 \mapsto \int_{\partial D} v(x)\partial_{\nu_x} u(x, x_0)ds(x)\right], \tag{3.20}$$

with $x_0 \in C$ and $u(\cdot, x_0) \in U$, has a dense range.

Proof. It suffices to prove that the transpose operator

$${}^tM \ : \ L^2(C) \to H^{-\frac{1}{2}}(\partial D), \quad \varphi \overset{{}^tM}{\mapsto} \left[x \mapsto \int_C \varphi(x_0)\partial_{\nu_x} u(x, x_0)ds(x_0)\right] \tag{3.21}$$

(with $x \in \partial D$) is injective. Let $\varphi \in L^2(C)$ such that ${}^tM\varphi = 0$. For each $x \in \mathbb{R}^2$ we can define the function v as

$$v(x) := \int_C \varphi(x_0)u(x, x_0)ds(x_0). \tag{3.22}$$

Since $u(\cdot, x_0)$ verifies (3.1), it follows that v satisfies $\Delta v + \tilde{k}_b^2(x)v = 0$ in $\mathbb{R}^2 \setminus C$; moreover, according to (3.1), $u = u^i + u^s$, where the incident field is $u^i(x, x_0) := G_b(x, x_0)$ and $u^s(x, x_0)$ is the corresponding scattered field. Then, v can be regarded as the total field $v = v^i + v^s$ resulting from the sum of the incident field $v^i(x) := \int_C \varphi(x_0)G_b(x, x_0)ds(x_0)$ for $x \in \mathbb{R}^2$, which is the single-layer potential of density φ and satisfies

$$\Delta v + k_b^2(x)v = 0 \tag{3.23}$$

in $\mathbb{R}^2 \setminus C$, and the scattered field $v^s(x) := \int_C \varphi(x_0)u^s(x, x_0)ds(x_0)$ for $x \in \mathbb{R}^2$, which verifies (3.23) in $\mathbb{R}^2 \setminus \overline{D}$. Moreover, by virtue of (3.21) and (3.22), it holds $\partial_\nu v = {}^tM\varphi$, but ${}^tM\varphi = 0$ by assumption: then, it turns out that the function v given by (3.22) is the unique solution of the following boundary value problem: $\Delta v + k_D^2(x)v = 0$ in D and $\partial_\nu v = 0$ on ∂D. Hence $v = 0$ in D and by the unique continuation principle $v = 0$ in V, i.e. $v^s = -v^i$ in V. If we now define $\tilde{v}^s$ in $\mathbb{R}^2$ as $\tilde{v}^s(x) := v^s(x)$ for $x \in \mathbb{R}^2 \setminus \overline{D}$ and $\tilde{v}^s(x) := -v^i(x)$ for $x \in \overline{D}$, we can easily see that $\tilde{v}^s$ is an entire radiating solution of (3.23). As a consequence [13], we have $\tilde{v}^s = 0$ in $\mathbb{R}^2$, and then $v^i = 0$ in V. In particular, the single-layer potential of density φ is null on C, and since the single-layer operator is injective (see Theorem A.2), then $\varphi = 0$, ${}^tM$ is injective and M has a dense range. □

LEMMA 3.5. *For each $f \in H^{\frac{1}{2}}(\partial D)$, the set $E_f := \{\partial_\nu u : u \in H^1_\Delta(D)$ and $u|_{\partial D} = f\}$ is dense in $H^{-\frac{1}{2}}(\partial D)$.*

Proof. We firstly observe that E_f is an affine space, i.e. $E_f = E_0 + \partial_\nu u_f$, where $u_f \in H^1_\Delta(D)$ is the unique solution of the following boundary value problem: $\Delta u = 0$

in D and $u = f$ on ∂D. Then, in order to prove that E_f is dense in $H^{-\frac{1}{2}}(\partial D)$, it suffices to show this property for E_0. Indeed, let us assume that E_0 is dense in $H^{-\frac{1}{2}}(\partial D)$ and let v be any element of $H^{-\frac{1}{2}}(\partial D)$: then, $v - \partial_\nu u_f \in H^{-\frac{1}{2}}(\partial D)$. Hence, for every $\epsilon > 0$, there exists $w^\epsilon \in E_0$ such that $\|w^\epsilon - (v - \partial_\nu u_f)\|_{H^{-\frac{1}{2}}(\partial D)} = \|v - (w^\epsilon + \partial_\nu u_f)\|_{H^{-\frac{1}{2}}(\partial D)} < \epsilon$, i.e. we have found $w^\epsilon + \partial_\nu u_f \in E_f$ that approximates $v \in H^{-\frac{1}{2}}(\partial D)$.

Now, in order to show that E_0 is dense, it suffices to prove the density of the range of the operator $T : L^2(D) \to H^{-\frac{1}{2}}(\partial D)$, defined as $T\varphi := \partial_\nu u_\varphi$, where, for all $\varphi \in L^2(D)$, $u_\varphi \in H^1_\Delta(D)$ is the unique solution of the boundary value problem $\Delta u = \varphi$ in D and $u = 0$ on ∂D. We can prove the density of the range of T by proving that its transpose ${}^tT$ is injective. Then, we firstly show that ${}^tT : H^{\frac{1}{2}}(\partial D) \to L^2(D)$ is given by ${}^tTg = w_g$, where $w_g \in H^1_\Delta(D)$ is the unique solution of the boundary value problem $\Delta w = 0$ in D and $w = g$ on ∂D. By using the second Green's identity in D and remembering that $T\varphi = \partial_\nu u_\varphi$, as well as the boundary value problems solved by u_φ and w_g, we find that $\forall g \in H^{\frac{1}{2}}(\partial D)$ and $\forall \varphi \in L^2(D)$ it holds:

$$\int_{\partial D} g(x)(T\varphi)(x)ds(x) = \int_{\partial D} w_g(x)\partial_\nu u_\varphi(x)ds(x) = \int_D w_g(x)\varphi(x)dx. \tag{3.24}$$

The equality between the first and the last term of (3.24) now shows that ${}^tTg = w_g$, as claimed. Now, let us consider $g \in H^{\frac{1}{2}}(\partial D)$ such that ${}^tTg = 0$: by uniqueness of the solution to the Laplace equation for a Dirichlet boundary condition on ∂D, we have $g = 0$. Hence ${}^tT$ is injective, i.e. T has a dense range. □

The following theorem uses notations and results described in Appendix B.

THEOREM 3.6. *The operator P is bounded. Moreover, if k_0 is not a transmission eigenvalue of the following problem*

$$\begin{cases} \Delta v + k^2 n_1(k) v = 0 & \text{in } D \\ \Delta u + k^2 n_D(k)(x) u = 0 & \text{in } D \\ (v - u) = 0 & \text{on } \partial D \\ \partial_\nu (v - u) = 0 & \text{on } \partial D, \end{cases} \tag{3.25}$$

then the operator P is injective and has a dense range.

Proof. We split the proof into three steps.

Step 1: P is bounded. Since $u(\cdot, x_0)$ is singular only for $x = x_0$, we have that $u(\cdot,\cdot) \in L^\infty(D \times C) \subset L^2(D \times C)$. Then, remembering definition (3.7), the boundedness of $k_D \in L^\infty(D)$ and the Cauchy-Schwarz inequality, we have $\|Pv\|^2_{L^2(C)} \leq \left\|k_1^2 - k_D^2\right\|^2_{L^\infty(D)} \|v\|^2_{L^2(D)} \|u\|^2_{L^2(D\times C)}$. We observe that since the $L^2(D)$-norm is bounded by the $H^0_\Delta(D)$-norm, this inequality shows the boundedness of P whichever of the two norms is chosen for its domain K^0_1.

Step 2: P is injective. Let $v \in K^0_1$ be such that $Pv = 0$. Then, recalling definition (3.7), we have:

$$\int_D \left[k_1^2 - k_D^2(x)\right] u(x, x_0) v(x) dx = 0 \quad \forall x_0 \in C. \tag{3.26}$$

By Lemma 3.3, the set $U = \{u(\cdot, x_0) : x_0 \in C\}$ is dense in K^1_D with respect to the $L^2(D)$-norm: from (3.26) and the continuity of the scalar product in L^2, we then have

$$\int_D \left[k_1^2 - k_D^2(x)\right] u(x) v(x) dx = 0 \quad \forall u \in K^1_D. \tag{3.27}$$

For the same $v \in K_1^0$, consider now the unique solution $w \in H_\Delta^1(D)$ of

$$\begin{cases} \Delta w + k_D^2(x)w = [k_1^2 - k_D^2(x)]v & \text{in } D \\ w = 0 & \text{on } \partial D. \end{cases} \tag{3.28}$$

Since $u \in K_D^1$ and w verifies the first of (3.28), by virtue of (3.27) we can show that

$$-\int_D \Delta u(x)w(x)dx + \int_D \Delta w(x)u(x)dx = \int_D \left[k_1^2 - k_D^2(x)\right] u(x)v(x)dx = 0 \quad \forall u \in K_D^1. \tag{3.29}$$

Then, the second Green's identity in D, with $w = 0$ on ∂D by (3.28), yields

$$\int_{\partial D} u(x)\partial_\nu w(x)ds(x) = 0 \quad \forall u \in K_D^1. \tag{3.30}$$

We now observe that, for each $f \in H^{\frac{1}{2}}(\partial D)$, there exists a unique solution $u_f \in K_D^1$ to the following boundary value problem: $\Delta u + k_D^2(x)u = 0$ in D and $u = f$ on ∂D. As a consequence, $\{u|_{\partial D} : u \in K_D^1\} = H^{\frac{1}{2}}(\partial D)$ and then, by virtue of (3.30), we get $\int_{\partial D} f(x)\partial_\nu w(x)ds(x) = 0 \ \forall f \in H^{\frac{1}{2}}(\partial D)$, which proves that $\partial_\nu w = 0$. Consider now the function $u \in H_\Delta^0(D)$ defined as $u := w + v$. Remembering that w is the solution of (3.28), $\partial_\nu w = 0$ and $v \in K_1^0$, it is easy to realize that v and u satisfy the homogeneous transmission problem (3.25) for $k = k_0$. Since we have supposed that k_0 is not a transmission eigenvalue, this implies that $u = v = 0$; then P is injective.

Step 3: P has a dense range. Let $h \in L^2(C)$ and $\epsilon > 0$: by virtue of Lemma 3.4, there exists $f \in H^{\frac{1}{2}}(\partial D)$ such that

$$\|Mf - h\|_{L^2(C)} < \frac{\epsilon}{2}. \tag{3.31}$$

Moreover the operator Q defined as

$$Q \ : \ H^{-\frac{1}{2}}(\partial D) \to L^2(C), \quad v \overset{Q}{\mapsto} \left[x_0 \mapsto \int_{\partial D} v(x)u(x, x_0)dx\right] \tag{3.32}$$

(with $u(\cdot, x_0) \in U$) is easily seen to be bounded. By virtue of Lemma 3.5, there exists a function $q \in H_\Delta^1(D)$ such that $q|_{\partial D} = f$ and

$$\|\partial_\nu q\|_{H^{-\frac{1}{2}}(\partial D)} < \frac{\epsilon}{2\,\|Q\|}. \tag{3.33}$$

Since we have supposed that k_0 is not a transmission eigenvalue (see Appendix B), there exist $\tilde{v}, \tilde{w} \in H_\Delta^0(D)$ such that $\tilde{v} - \tilde{w} \in H_\Delta^1(D)$ and

$$\begin{cases} \Delta\tilde{v} + k_0^2 n_1(k_0)\tilde{v} = 0 & \text{in } D \\ \Delta\tilde{w} + k_0^2 n_D(k_0)(x)\tilde{w} = 0 & \text{in } D \\ (\tilde{v} - \tilde{w}) = q & \text{on } \partial D \\ \partial_\nu(\tilde{v} - \tilde{w}) = \partial_\nu q & \text{on } \partial D. \end{cases} \tag{3.34}$$

Let $\tilde{u} := \tilde{v} - \tilde{w}$. Then $\tilde{u} \in H_\Delta^1(D)$, and from the first two equations in (3.34) we have $\Delta\tilde{u} + k_D^2(x)\tilde{u} = -\left[k_1^2 - k_D^2(x)\right]\tilde{v}$ in D. Then, by virtue of the previous equation and the second Green's identity in D, we have that for all $u \in K_D^1$ it holds $\int_D \left[k_1^2 - k_D^2(x)\right] u(x)\tilde{v}(x)dx = \int_{\partial D} \tilde{u}(x)\partial_\nu u(x)ds(x) - \int_{\partial D} u(x)\partial_\nu\tilde{u}(x)ds(x)$, i.e., remembering also that $\tilde{u} = \tilde{v} - \tilde{w}$, $q|_{\partial D} = f$ and the boundary conditions in (3.34),

$\int_D \left[k_1^2 - k_D^2(x)\right] u(x)\tilde{v}(x)dx = \int_{\partial D} f(x)\partial_\nu u(x)ds(x) - \int_{\partial D} u(x)\partial_\nu q(x)ds(x)$. If we now remember definitions (3.7), (3.20) and (3.32), we can rewrite the last equation as $(Pv)(x_0) = (Mf)(x_0) - (Q\partial_\nu q)(x_0)\ \forall x_0 \in C$; then, by using the triangle inequality and recalling inequalities (3.31), (3.33), we get $\|Pv - h\|_{L^2(C)} \leq \|Mf - h\|_{L^2(C)} + \|Q\|\,\|\partial_\nu q\|_{L^2(\partial D)} < \epsilon$, which shows that P has a dense range, since h is arbitrarily chosen in $L^2(C)$. □

COROLLARY 3.7. *If k_0 is not a transmission eigenvalue of problem (3.25), then the operator $F = -PH$ is injective and has a dense range.*

Proof. The injectivity of F is obvious. As regards the denseness of its range, let us consider any $w \in L^2(C)$: by using the triangle inequality, the linearity and the boundedness of the operator P (see Theorem 3.6), and remembering that both P and H have a dense range, it turns out that for each $\epsilon > 0$ we can find $g \in H^{-\frac{1}{2}}(C)$ (and an auxiliary $v \in K_1^0$) such that $\|w - (-PHg)\|_{L^2(C)} \leq \|w - Pv\|_{L^2(C)} + \|P(v + Hg)\|_{L^2(C)} < \epsilon/2 + \|P\|\,\|v + Hg\|_{L^2(D)} < \epsilon/2 + \|P\|\epsilon/(2\|P\|) = \epsilon$. □

Point 4.

In order to characterize the range of P, for each $z \in \Omega$ we introduce the function $\Lambda_z \in L^2(C)$ defined as

$$\Lambda_z \ : \ C \to \mathbb{C}, \quad x_0 \overset{\Lambda_z}{\mapsto} \mathcal{R}(u(\cdot, x_0), G_z). \tag{3.35}$$

Then the following theorem, again based on results in Appendix B, holds.

THEOREM 3.8. *Suppose that k_0 is not a transmission eigenvalue of problem (3.25). Then, for all $z \in \Omega$, $\Lambda_z \in range(P)$ if and only if $z \in D$.*

Proof. 1) Let $z \in D$ and let us consider a function $\beta \in C^\infty(\Omega)$ such that [20] $\beta = 0$ in a neighbourhood of z and $\beta = 1$ in a neighbourhood of ∂D: then $\beta G_z \in H^1_\Delta(D)$. Since k_0 is not a transmission eigenvalue of problem (3.25), there exist (see Appendix B) $\tilde{v}, \tilde{w} \in H^0_\Delta(D)$ such that $\tilde{v} - \tilde{w} \in H^1_\Delta(D)$ and

$$\begin{cases} \Delta\tilde{v} + k_0^2 n_1(k_0)\tilde{v} = 0 & \text{in } D \\ \Delta\tilde{w} + k_0^2 n_D(k_0)(x)\tilde{w} = 0 & \text{in } D \\ (\tilde{v} - \tilde{w}) = \beta G_z & \text{on } \partial D \\ \partial_\nu(\tilde{v} - \tilde{w}) = \partial_\nu(\beta G_z) & \text{on } \partial D. \end{cases} \tag{3.36}$$

Since $\beta = 1$ in a neighbourhood of ∂D, the factor β can be omitted in the boundary conditions of (3.36). Moreover, since $z \in D$, both G_z and $u(\cdot, x_0) \in U$ are in $H^1_\Delta(\Omega\backslash\overline{D})$ and satisfy equation (3.9) in $\Omega\backslash\overline{D}$; hence, if we put $\tilde{u} := \tilde{v} - \tilde{w}$, by applying the second Green's identity in $\Omega \setminus \overline{D}$ and remembering definition (3.7), as well as the boundary conditions of (3.36), we get:

$$\begin{aligned} \mathcal{R}(u(\cdot, x_0), G_z) &= -\int_{\partial D} G_z(x)\partial_{\nu_x} u(x, x_0)ds(x) + \int_{\partial D} u(x, x_0)\partial_{\nu_x} G_z(x)ds(x) = \\ &= -\int_D \left[k_1^2 - k_D^2(x)\right] u(x, x_0)\tilde{v}(x)dx = -(P\tilde{v})(x_0) \quad \forall x_0 \in C, \end{aligned} \tag{3.37}$$

i.e., recalling definition (3.35), $\Lambda_z(x_0) = [P(-\tilde{v})](x_0)$ for all $x_0 \in C$: this means that $\Lambda_z \in range(P)$.

2) Let us now suppose that $z \in \Omega \setminus \overline{D}$ and, by contradiction, that $\Lambda_z \in range(P)$. By definition (3.2) and recalling from (3.1) that $u = u^s + u^i$ with $u^i(\cdot, x_0) = G_b(\cdot, x_0)$,

for all $x_0 \in C$ we have

$$\mathcal{R}(u(\cdot,x_0),G_z) = \int_\Gamma [u^s(x,x_0)\partial_{\nu_x}G(x,z) - G(x,z)\partial_{\nu_x}u^s(x,x_0)]\,ds(x) + \\ + \int_\Gamma [G_b(x,x_0)\partial_{\nu_x}G(x,z) - G(x,z)\partial_{\nu_x}G_b(x,x_0)]\,ds(x). \tag{3.38}$$

We now observe that, for $x \in \Gamma = \partial\Omega$ and $x_0 \in C$, $G_b(\cdot,x_0)$ solves equation (3.9) in Ω, while the Green's function for (3.9) is just $G(\cdot,z)$: then, by applying Green's representation formula [20] to $G_b(\cdot,x_0)$, we find:

$$\mathcal{R}(u(\cdot,x_0),G_z) = \int_\Gamma [u^s(x,x_0)\partial_{\nu_x}G(x,z) - G(x,z)\partial_{\nu_x}u^s(x,x_0)]\,ds(x) - G_b(x_0,z). \tag{3.39}$$

Now, for $x_0 \in \mathbb{R}^2 \setminus \overline{D}$, let us define

$$v(x_0) := \int_\Gamma [u^s(x,x_0)\partial_{\nu_x}G(x,z) - G(x,z)\partial_{\nu_x}u^s(x,x_0)]\,ds(x). \tag{3.40}$$

By reciprocity, for all $x \in \Gamma$, $u^s(x,\cdot)$ is a radiating solution of

$$\Delta u + k_b^2(x_0)u = 0 \tag{3.41}$$

in $\mathbb{R}^2 \setminus \overline{D}$ with respect to the variable x_0; as a consequence, v too is a radiating solution in $\mathbb{R}^2 \setminus \overline{D}$ of the same equation. Moreover, by virtue of (3.39) and (3.40), it holds:

$$\mathcal{R}(u(\cdot,x_0),G_z) = v(x_0) - G_b(x_0,z) \quad \forall x_0 \in C. \tag{3.42}$$

Since we have supposed that $\Lambda_z \in range(P)$, there exists $w \in K_1^0$ such that

$$\mathcal{R}(u(\cdot,x_0),G_z) = \int_D \left[k_1^2 - k_D^2(x)\right] w(x)u(x,x_0)dx \quad \forall x_0 \in C. \tag{3.43}$$

Now, let $\tilde{v}$ be the function defined for all $x_0 \in \mathbb{R}^2 \setminus \overline{D}$ as

$$\tilde{v}(x_0) := \int_D \left[k_1^2 - k_D^2(x)\right] w(x)u(x,x_0)dx. \tag{3.44}$$

Then, by reciprocity, $\tilde{v}$ is a radiating solution of (3.41) in $\mathbb{R}^2 \setminus \overline{D}$. Moreover, by (3.43) and (3.44), we have

$$\mathcal{R}(u(\cdot,x_0),G_z) = \tilde{v}(x_0) \quad \forall x_0 \in C. \tag{3.45}$$

Now, from (3.42) and (3.45), it follows that $\tilde{v}$ and $v - G_b(\cdot,z)$ coincide on C. Moreover, since $\tilde{v}$ and $v - G_b(\cdot,z)$ are radiating solutions of (3.41) in $\mathbb{R}^2 \setminus \overline{V}$, by Theorem A.1 they coincide in $\mathbb{R}^2 \setminus \overline{V}$. Then, by virtue of the unique continuation principle, they coincide in $\mathbb{R}^2 \setminus (\overline{D} \cup \{z\})$. Nonetheless, $\tilde{v}$ is regular in z whereas $v - G_b(\cdot,z)$ is not, which is a contradiction. □

Point 5.

We can now carry out the last point of our workplan, by proving in the next theorem the existence of approximate (in $L^2(C)$) solutions of equation (3.3).

THEOREM 3.9. *Suppose that k_0 is not a transmission eigenvalue of problem (3.25) and let $z \in \Omega$. Then:*

a) if $z \in D$, for any given $\epsilon > 0$ there exists a $g_z^\epsilon \in H^{-\frac{1}{2}}(C)$ such that

$$\left\|\mathcal{R}(u(\cdot,\cdot), s_{g_z^\epsilon}) - \mathcal{R}(u(\cdot,\cdot), G_z)\right\|_{L^2(C)} < \epsilon \tag{3.46}$$

(where $u(\cdot,\cdot)$ is simply obtained by $u(\cdot, x_0) \in U$ when $x_0 \in C$ is regarded as a variable) and $s_{g_z^\epsilon}$ converges in $L^2(D)$ as $\epsilon \to 0$; moreover, for any fixed $\epsilon > 0$, every $g_z^\epsilon \in H^{-\frac{1}{2}}(C)$ verifying inequality (3.46) is such that

$$\lim_{z\to\partial D} \left\|s_{g_z^\epsilon}\right\|_{L^2(D)} = \infty \quad \text{and} \quad \lim_{z\to\partial D} \|g_z^\epsilon\|_{H^{-\frac{1}{2}}(C)} = \infty; \tag{3.47}$$

b) if $z \in \Omega \setminus \overline{D}$, for any given $\epsilon > 0$ there exists a $g_z^\epsilon \in H^{-\frac{1}{2}}(C)$ such that

$$\left\|\mathcal{R}(u(\cdot,\cdot), s_{g_z^\epsilon}) - \mathcal{R}(u(\cdot,\cdot), G_z)\right\|_{L^2(C)} < \epsilon; \tag{3.48}$$

moreover, every $g_z^\epsilon \in H^{-\frac{1}{2}}(C)$ verifying inequality (3.48) is such that

$$\lim_{\epsilon\to 0} \left\|s_{g_z^\epsilon}\right\|_{L^2(D)} = \infty \quad \text{and} \quad \lim_{\epsilon\to 0} \|g_z^\epsilon\|_{H^{-\frac{1}{2}}(C)} = \infty. \tag{3.49}$$

Proof. *a)* Let $z \in D$: then, according to Theorem 3.8, $\Lambda_z \in \mathit{range}(P)$: in fact, $\Lambda_z = P(-\tilde{v})$, see (3.37). Since the range of H is dense in K_1^0 with respect to the $L^2(D)$-norm (by Theorem 3.2) and $\tilde{v} \in K_1^0$ (see the first equation of (3.36)), for any given $\epsilon' > 0$ there exists $g_z^{\epsilon'} \in H^{-\frac{1}{2}}(C)$ such that

$$\left\|Hg_z^{\epsilon'} - \tilde{v}\right\|_{L^2(D)} < \epsilon'. \tag{3.50}$$

Hence, recalling the factorization $F = -PH$ given by Theorem 3.1, the boundedness of P and the equality $\Lambda_z = P(-\tilde{v})$, we have

$$\left\|Fg_z^{\epsilon'} - \Lambda_z\right\|_{L^2(C)} = \left\|-PHg_z^{\epsilon'} + P\tilde{v}\right\|_{L^2(C)} \le \|P\| \left\|Hg_z^{\epsilon'} - \tilde{v}\right\|_{L^2(D)} \tag{3.51}$$

and then, by using (3.50), (3.51) and choosing $\epsilon' = \epsilon/\|P\|$, we find $\|Fg_z^\epsilon - \Lambda_z\|_{L^2(C)} < \epsilon$, which, by virtue of definitions (3.5) and (3.35), is exactly thesis (3.46). The convergence of $s_{g_z^\epsilon}$ in $L^2(D)$ as $\epsilon \to 0$ immediately follows from the definition (3.6) of H and inequality (3.50).

In order to prove limits (3.47), we firstly remember equality (3.37), i.e. $\Lambda_z = P(-\tilde{v})$, where $(\tilde{v}, \tilde{w})$ is the solution of (3.36). Then, we define the function $\tilde{u}$ as $\tilde{u} := \tilde{v} - \tilde{w}$ in D and $\tilde{u} := G_z$ in $\mathbb{R}^2 \setminus \overline{D}$. Since $\tilde{v} - \tilde{w} = G_z$ and $\partial_\nu(\tilde{v} - \tilde{w}) = \partial_\nu G_z$ on ∂D, then $\tilde{u}$ is in $H^1_{\mathrm{loc}}(\mathbb{R}^2)$ and is the solution of the following scattering problem:

$$\begin{cases} \Delta u + \tilde{k}^2(x)u = \left[\tilde{k}^2(x) - k^2(x)\right]\tilde{v} \quad \text{in} \quad \mathbb{R}^2 \\ \lim\limits_{r\to\infty} \sqrt{r}(\partial_r u - \mathrm{i}k_0 u) = 0; \end{cases} \tag{3.52}$$

we recall that $k^2(x)$ and $\tilde{k}^2(x)$ are defined in (2.4) and (2.5) respectively. Moreover, by continuity of the solution with respect to initial data, for all $R > 0$ such that D is included in the open ball of center O and radius R, there exists a constant $\alpha_R \in \mathbb{R}_+^*$ (which depends on R and $\tilde{k}(x)$) such that for all $h \in L^2(D)$, the solution u of the scattering problem $\Delta u + \tilde{k}^2(x)u = h$ in $\mathbb{R}^2$, with $\lim_{r\to\infty} \sqrt{r}(\partial_r u - \mathrm{i}k_0 u) = 0$, verifies

$\|u\|_{H^1(B_R)} \leq \alpha_R \|h\|_{L^2(D)}$. Then, coming back to problem (3.52), we can easily deduce that

$$\|G_z\|_{H^1(B_R\setminus\overline{D})} \leq \alpha_R \|\tilde{v}\|_{L^2(D)}. \tag{3.53}$$

Although the Green's function G_z describes the inhomogeneous background in Ω, by superposition (analogously to relation (2.6)) its singularity in z is only determined by the Green's function of the medium (in our case, the tumor) in which z is located: in particular, $G_z \notin H^1(A)$ for any $A \subset \mathbb{R}^2$ such that $z \in \overline{A}$ [7]. Hence, from (3.53), we find that $\lim_{z\to\partial D} \|\tilde{v}\|_{L^2(D)} = \infty$ and consequently, by virtue of (3.50), $\lim_{z\to\partial D} \|Hg_z^\epsilon\|_{L^2(D)} = \infty$, which, remembering definition (3.6), is just the first limit in (3.47). Finally, the boundedness of H (i.e. of the single layer potential [20]) implies that $\lim_{z\to\partial D} \|g_z^\epsilon\|_{H^{-\frac{1}{2}}(C)} = \infty$, i.e. the second limit in (3.47).

b) Let $z \in \Omega\setminus\overline{D}$. Since P has a dense range and $\Lambda_z \in \overline{range(P)}\setminus range(P)$, we can use Tikhonov regularization [25] to show that there exists a sequence $\{f_{z,p}\}_{p=1}^\infty \subset K_1^0$ such that (see [2, 16])

$$\lim_{p\to\infty} \|-Pf_{z,p} - \Lambda_z\|_{L^2(C)} = 0 \quad \text{and} \quad \lim_{p\to\infty} \|f_{z,p}\|_{L^2(D)} = \infty. \tag{3.54}$$

In particular, the first limit in (3.54) implies that, for each $\epsilon > 0$, there exists $\tilde{p} \equiv \tilde{p}(\epsilon)$ such that $f_z^\epsilon := f_{z,\tilde{p}} \in K_1^0$ satisfies

$$\|-Pf_z^\epsilon - \Lambda_z\|_{L^2(C)} < \frac{\epsilon}{2}. \tag{3.55}$$

Moreover, since H has a dense range, for each $\epsilon > 0$ there exists $g_z^\epsilon \in H^{-\frac{1}{2}}(C)$ such that

$$\|Hg_z^\epsilon - f_z^\epsilon\|_{L^2(D)} < \frac{\epsilon}{2\|P\|}. \tag{3.56}$$

Then, by using the triangle inequality, relations (3.55), (3.56) and recalling that $F = -PH$, we get:

$$\begin{aligned}\|Fg_z^\epsilon - \Lambda_z\|_{L^2(C)} = \|PHg_z^\epsilon + \Lambda_z\|_{L^2(C)} \leq \|Pf_z^\epsilon - PHg_z^\epsilon\|_{L^2(C)} + \|Pf_z^\epsilon + \Lambda_z\|_{L^2(C)} < \\ < \|P\|\frac{\epsilon}{2\|P\|} + \frac{\epsilon}{2} = \epsilon,\end{aligned} \tag{3.57}$$

so that inequality (3.48) is verified. Now, let us assume, by contradiction, that there exists a non-divergent sequence $\{f_{z,p}\}_{p=1}^\infty \subset K_1^0$ verifying the first limit in (3.54). Then, we can extract from $\{f_{z,p}\}_{p=1}^\infty$ a subsequence $\{f_{z,q} \equiv f_{z,p(q)}\}_{q=1}^\infty$ that is bounded in $L^2(D)$. Since $\{f_{z,q}\}_{q=1}^\infty$ is bounded, we can in turn extract from it a subsequence $\{f_{z,r} \equiv f_{z,q(r)}\}_{r=1}^\infty$ that is weakly convergent to a certain element $f_z^* \in K_0^1$. The continuity of P then implies that $-Pf_{z,r}$ weakly converges to $-Pf_z^*$; on the other hand, from the first limit in (3.54) we know that $-Pf_{z,r}$ strongly converges to Λ_z in $L^2(C)$: as a consequence, we obtain that $-Pf_z^* = \Lambda_z$, i.e. Λ_z is in the range of P, in contradiction with Theorem 3.8. If we now use this argument with a sequence of the kind $\{f_{z,p}\}_{p=1}^\infty := \{s_{g_{z,p}}\}_{p=1}^\infty$ (as made possible by the density of the range of $F = -PH$, see Corollary 3.7), we can easily prove the first limit in (3.49). Finally, as in the previous case *a*), the boundedness of the operator H implies the second limit in (3.49). □

4. The visualization algorithm. The goal of the present section is to show how to visualize breast tumors by using the RGF equation (3.3) as a tool to compute an indicator function, as suggested by Theorem 3.9. The traditional pointwise algorithm presented in [8, 9] takes inspiration from blowing-up limits analogous to those in (3.47) and (3.49), and consists in plotting, for each z belonging to a numerical grid covering the sampling region Ω, a Tikhonov regularized solution of (3.3).

We first observe that in real experiments one needs to perform an angular discretization involving the positions of both the antennas on C sending the incident waves and the antennas on Γ measuring the total electric field and its normal derivative. For sake of simplicity, we discretize the continuous parameters x_Γ on Γ and y_C on C with the same number N of equispaced knots, choosing C and Γ as concentric circles of radii R_C and R_Γ respectively; in particular, we now have $\Omega = \{z \in \mathbb{R}^2 \,:\, |z| < R_\Gamma\}$. Moreover, each of the pairs of discretization points $\{(x_0, y_0), \ldots, (x_{N-1}, y_{N-1})\}$ is assumed to belong to a radius of C, i.e. the (pointlike) emitting and receiving antennas are in a radial symmetry (we notice that relaxing these assumptions would not change the general scheme of the following visualization algorithm, but would make the new formulation more complicated). The discretized form of (3.3) can be written in a compact form by establishing the following notations for each $i, j = 0, \ldots, N-1$ and for each $z \in \Omega$:

$$\begin{aligned} U_{ij} &:= u(x_i, y_j), \quad L_{ij} := \frac{\partial G}{\partial \nu(x)}(x_i, y_j), \quad g_j := g(y_j), \quad G_{ij} := G(x_i, y_j), \\ V_{ij} &:= \frac{\partial u}{\partial \nu(x)}(x_i, y_j), \quad l_i(z) := \frac{\partial G}{\partial \nu(x)}(x_i, z), \quad q_i(z) := G(x_i, z). \end{aligned} \tag{4.1}$$

We now regard the quantities U_{ij}, L_{ij}, G_{ij}, V_{ij} as the entries of the square $N \times N$ matrices $\mathbf{U}$, $\mathbf{L}$, $\mathbf{G}$, $\mathbf{V}$ respectively, while we consider g_j, $l_i(z)$, $q_i(z)$ as the N components of the column vectors $\mathbf{g}$, $\mathbf{l}(z)$, $\mathbf{q}(z)$; finally, using the common matrix transposition and the rows $\times$ columns product, we put, for all $z \in \Omega$,

$$\boldsymbol{\Delta}\mathbf{s} := \mathrm{diag}(\Delta s_j) \equiv \frac{2\pi R_C}{N}\mathbf{I}_N, \quad \mathbf{D} := \mathbf{U}^{\mathrm{T}}\mathbf{L} - \mathbf{V}^{\mathrm{T}}\mathbf{G}, \quad \mathbf{b}(z) := \mathbf{U}^{\mathrm{T}}\mathbf{l}(z) - \mathbf{V}^{\mathrm{T}}\mathbf{q}(z), \tag{4.2}$$

where $\mathbf{I}_N$ is the identity matrix of order N and $\frac{2\pi R_C}{N}$ is the (constant) discretization step $\Delta s_j > 0$ over C $\forall j = 0, \ldots, N-1$. With the previous notations, the discretized version of (3.3) is the one-parameter family of linear systems in the (z-dependent) unknown $\mathbf{g} = \mathbf{g}(z)$

$$\mathbf{D}\,\boldsymbol{\Delta}\mathbf{s}\,\mathbf{g}(z) = \mathbf{b}(z) \quad \forall z \in \Omega. \tag{4.3}$$

From now on, we shall denote with $\mathbb{C}^N_{\boldsymbol{\Delta}\mathbf{s}}$ the vector space $\mathbb{C}^N$ equipped with the $\boldsymbol{\Delta}\mathbf{s}$-weighted scalar product, defined as $(\mathbf{x}, \mathbf{y})_{\boldsymbol{\Delta}\mathbf{s}, \mathbb{C}^N} := \sum_{j=1}^N x_j\, \Delta s_j\, \bar{y}_j$ for all $\mathbf{x}, \mathbf{y} \in \mathbb{C}^N$; this scalar product naturally induces a norm denoted with $\|\cdot\|_{\boldsymbol{\Delta}\mathbf{s}, \mathbb{C}^N}$. Then we shall regard the matrix $\mathbf{A} := \mathbf{D}\,\boldsymbol{\Delta}\mathbf{s}$ as the matrix representation of the linear operator $\mathcal{A} : \mathbb{C}^N_{\boldsymbol{\Delta}\mathbf{s}} \to \mathbb{C}^N_{\boldsymbol{\Delta}\mathbf{s}}$ such that $\mathcal{A}(\mathbf{x}) = \mathbf{D}\,\boldsymbol{\Delta}\mathbf{s}\,\mathbf{x}$ for all $\mathbf{x} \in \mathbb{C}^N_{\boldsymbol{\Delta}\mathbf{s}}$. We now point out that our simplified model for the healthy breast allows an analytic knowledge of the matrices $\mathbf{L}$ and $\mathbf{G}$, as well as of the column vectors $\mathbf{l}(z)$ and $\mathbf{q}(z)$, but for sake of brevity we shall omit these laborious computations. In the case of more complex models for the healthy breast, $\mathbf{L}$, $\mathbf{G}$, $\mathbf{l}(z)$ and $\mathbf{q}(z)$ can be determined numerically. On the other hand, the experimental data are collected in the matrices $\mathbf{U}$ and $\mathbf{V}$: then, in general, only their noisy versions $\tilde{\mathbf{U}}$ and $\tilde{\mathbf{V}}$ are known. As a consequence of

definitions (4.2), both the matrix $\mathbf{D}$ and the column vector $\mathbf{b}(z)$ should be replaced by their noisy versions $\mathbf{D}_h$ and $\mathbf{b}_\delta(z)$ in equation (4.3), which then becomes

$$\mathbf{A}_h\,\mathbf{g}(z) = \mathbf{b}_\delta(z) \quad \forall z \in \Omega, \tag{4.4}$$

having denoted with $\mathbf{A}_h := \mathbf{D}_h\,\mathbf{\Delta s}$ the matrix representation of the noisy version $\mathcal{A}_h$ of the linear operator $\mathcal{A}$. Here the subscripts h and δ refer to bounds on the noise level, as specified in the following.

To implement the same "no-sampling" approach already developed for the linear sampling method [3, 5], we replace (4.4) with the functional equation in $[L^2(\Omega)]^N = \bigoplus_{i=1}^N L^2(\Omega)$

$$[\mathsf{A}_h\mathbf{g}(\cdot)](\cdot) = \mathbf{b}_\delta(\cdot), \tag{4.5}$$

where the linear operator $\mathsf{A}_h : [L^2(\Omega)]^N \to [L^2(\Omega)]^N$ is defined as

$$[\mathsf{A}_h\mathbf{g}(\cdot)](\cdot) := \left\{ \sum_{j=0}^{N-1} (A_h)_{ij}\, g_j(\cdot) \right\}_{i=0}^{N-1} \qquad \forall \mathbf{g}(\cdot) = \{g_j(\cdot)\}_{j=0}^{N-1} \in [L^2(\Omega)]^N \tag{4.6}$$

and $(A_h)_{ij}$ are the entries of the noisy matrix $\mathbf{A}_h$ previously introduced. Here, we are regarding $[L^2(\Omega)]^N$ as a Hilbert space with the scalar product $(\mathbf{f}(\cdot),\mathbf{g}(\cdot))_{2,N} := \int_\Omega (\mathbf{f}(z),\mathbf{g}(z))_{\mathbf{\Delta s},\mathbb{C}^N}\,dz \;\forall \mathbf{f}(\cdot),\mathbf{g}(\cdot) \in [L^2(\Omega)]^N$, and the induced norm $\|\mathbf{f}(\cdot)\|_{2,N} := \sqrt{\int_\Omega \|\mathbf{f}(z)\|^2_{\mathbf{\Delta s},\mathbb{C}^N}\,dz}$.

The Tikhonov regularized solution $\mathbf{g}_\alpha(\cdot)$ of equation (4.5) can be explicitly computed by using the singular representation of the linear operator $\mathcal{A}_h$, whose singular system $\{\sigma_p^h; \mathbf{u}_p^h, \mathbf{v}_p^h\}_{p=0}^{r^h-1}$ is strictly related to that of the matrix $\mathbf{A}_h$ [5] (r^h is the rank of $\mathbf{A}_h$). By means of computations analogous to those of [3, 5], we find:

$$\mathbf{g}_\alpha(\cdot) = \sum_{p=0}^{r^h-1} \frac{\sigma_p^h}{(\sigma_p^h)^2+\alpha} \left\langle \mathbf{b}_\delta(\cdot), \mathbf{v}_p^h \right\rangle_{\mathbf{\Delta s},\mathbb{C}^N} \mathbf{u}_p^h, \tag{4.7}$$

where, for any $\mathbf{f}(\cdot) \in [L^2(\Omega)]^N$ and $\mathbf{w} \in \mathbb{C}^N_{\mathbf{\Delta s}}$, we have denoted with $\langle \mathbf{f}(\cdot), \mathbf{w}\rangle_{\mathbf{\Delta s},\mathbb{C}^N}$ the element of $L^2(\Omega)$ defined by $z \mapsto (\mathbf{f}(z),\mathbf{w})_{\mathbf{\Delta s},\mathbb{C}^N}$ f.a.a. $z \in \Omega$. The visualization method based on the analysis of the RGF equation is therefore:

1. compute (4.7) by using the singular system of $\mathcal{A}_h$;
2. fix a value α^* for the regularization parameter α by applying some optimality criterion;
3. choose a suitable continuous monotonic function $J : [0,\infty) \to \mathbb{R}$ and plot the indicator function $\Psi(z) = J\left(\|\mathbf{g}_{\alpha^*}(z)\|^2_{\mathbf{\Delta s},\mathbb{C}^N}\right)$ for $z \in \Omega$, where

$$\|\mathbf{g}_{\alpha^*}(z)\|^2_{\mathbf{\Delta s},\mathbb{C}^N} = \sum_{p=0}^{r^h-1} \frac{(\sigma_p^h)^2}{[(\sigma_p^h)^2+\alpha^*]^2} \left| \left(\mathbf{b}_\delta(z), \mathbf{v}_p^h\right)_{\mathbf{\Delta s},\mathbb{C}^N} \right|^2. \tag{4.8}$$

From now on this algorithm will be called the RGF method (in the present implementation we have chosen $J = -\ln$).

Item No. 2 is a critical step. It can be implemented by applying the generalized discrepancy principle [25], i.e. by finding the zero α^* of the generalized discrepancy

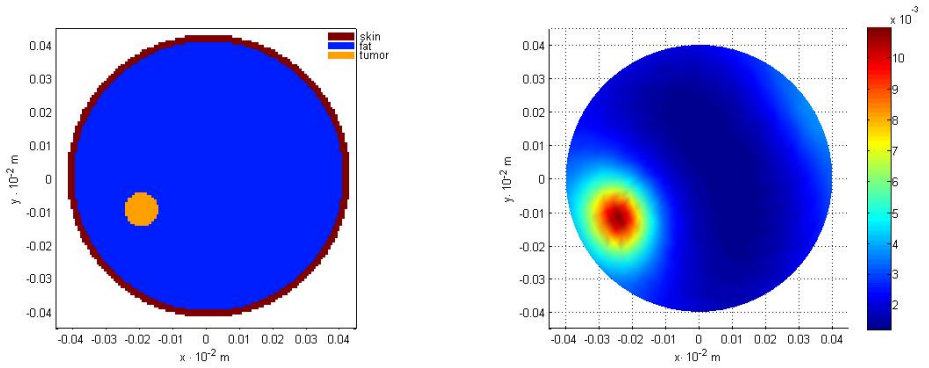

FIG. 5.1. *(a) Phantom of the breast: a circular tumor, centred in* $(-2.00, -1.00) \cdot 10^{-2}$ m *and with a diameter of* $1.00 \cdot 10^{-2}$ m*, is placed in the fat tissue. (b) Visualization provided by the RGF algorithm.*

function $\rho(\alpha) := \|[\mathsf{A}_h \mathbf{g}_\alpha(\cdot)](\cdot) - \mathbf{b}_\delta(\cdot)\|^2_{2,N} - (\delta + h\|\mathbf{g}_\alpha(\cdot)\|_{2,N})^2$, where we assume that noise bounds δ, h are known, such that $\|\mathbf{b}_\delta(\cdot) - \mathbf{b}(\cdot)\|_{2,N} \leq \delta$ and $\|\mathsf{A}_h - \mathsf{A}\| \leq h$. In the latter inequality, A denotes the noise-free version of A_h and $\|\cdot\|$ the operator norm: as in [3, 5], it is possible to prove that $\|\mathsf{A}_h - \mathsf{A}\| = \|\mathcal{A}_h - \mathcal{A}\| = |\sigma_0^h - \sigma_0|$, where σ_0 is the largest singular value of $\mathcal{A}$.

5. Applications to data. The purpose of this section is to validate the RGF visualization algorithm described above against synthetic near-fields in a microwave tomography experiment for breast cancer detection. The direct scattering data are computed by means of a standard method of moments code [22]. A set of $N = 16$ emitting antennas are placed on a circle surrounding the breast at a distance of $4.00 \cdot 10^{-2}$ m from the skin. The incident fields are TM-polarized cylindrical waves at a fixed frequency of 1.00 GHz. The scattered field is computed by the code, corrupted by 10% random Gaussian noise and then collected by $N = 16$ receiving antennas placed in a radial symmetry with respect to the emitters, on a circle at a distance of $3.00 \cdot 10^{-2}$ m from the skin. For all simulations, the computational time of our RGF inversion procedure is very short, i.e. around 1 s.

In order to perform our simulations, the values of the geometric and electric parameters characterizing the biological tissues (at a frequency of 1.00 GHz) are chosen in agreement with the realistic models given in [17], i.e.: skin: $\varepsilon_r = 4.09 \cdot 10^1$, $\sigma = 9.00 \cdot 10^{-1}$ S/m; fat: $\varepsilon_r = 1.00 \cdot 10^1$, $\sigma = 1.50 \cdot 10^{-1}$ S/m; tumor: $\varepsilon_r = 5.39 \cdot 10^1$, $\sigma = 7.00 \cdot 10^{-1}$ S/m; vein: $\varepsilon_r = 5.00 \cdot 10^1$, $\sigma = 1.70 \cdot 10^{-1}$ S/m; gland: $\varepsilon_r = 1.15 \cdot 10^1$, $\sigma = 1.70 \cdot 10^{-1}$ S/m. Our simplified model of the healthy breast consists of a disk representing the fat tissue, surrounded by a circular corona representing the skin: the radius of the disk is $5.00 \cdot 10^{-2}$ m and the thickness of the skin layer is $2.00 \cdot 10^{-3}$ m.

In the first numerical example, we place into the fat a circular tumor with a diameter of $1.00 \cdot 10^{-2}$ m: the corresponding phantom is represented in Fig. 5.1(a). Then, the RGF inversion algorithm is applied to the direct scattering data computed for this phantom, thus providing the reconstruction in Fig. 5.1(b).

The second simulation considers the same phantom as in Fig. 5.1, but now a square scatterer (with $\varepsilon_r = 2.00$, $\sigma = 1.50$ S/m) is placed outside the breast, as represented in Fig. 5.2(a). The reconstruction provided by the RGF method is shown in Fig. 5.2(b): the algorithm is robust with respect to the presence of outer scatterers,

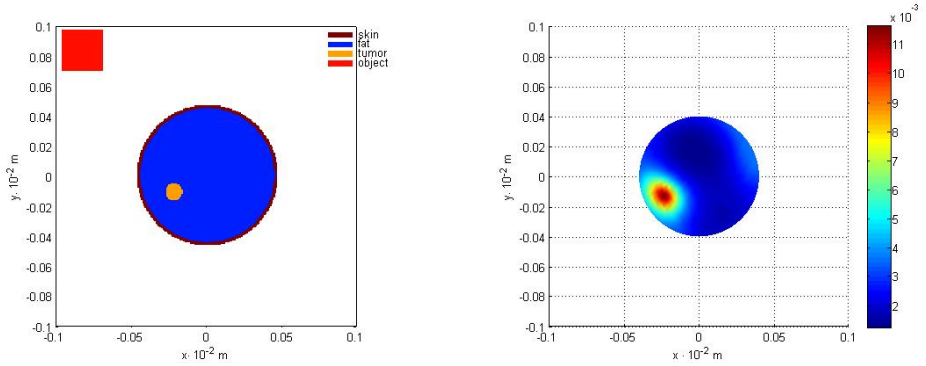

FIG. 5.2. *(a) Phantom of the breast: a circular tumor, centred in* $(-2.00, -1.00) \cdot 10^{-2}$ m *and with a diameter of* $1.00 \cdot 10^{-2}$ m*, is placed in the fat tissue; a square scatterer, centred in* $(-8.20, 8.20) \cdot 10^{-2}$ m *and with a side of* $2.75 \cdot 10^{-2}$ m *is put outside the breast. (b) Visualization provided by the RGF algorithm.*

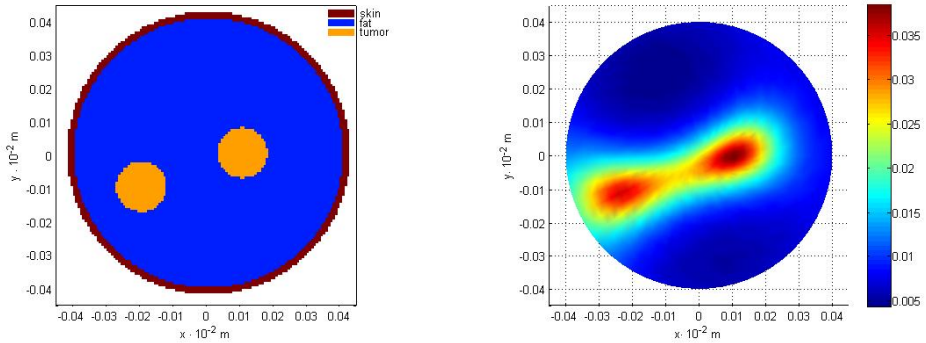

FIG. 5.3. *(a) Phantom of the breast: two circular tumors, with the same diameter of* $1.50 \cdot 10^{-2}$ m*, are placed in the fat tissue: one is centred in* $(-2.00, -1.00) \cdot 10^{-2}$ m*, the other in* $(1.00, 0.00) \cdot 10^{-2}$ m*. (b) Visualization provided by the RGF algorithm.*

although their presence is not encoded in the Green's function used to implement it.

In the third example, two circular tumors having the same diameter of $1.50 \cdot 10^{-2}$ m are placed at a distance of $3.16 \cdot 10^{-2}$ m between their centers, as illustrated in Fig. 5.3(a); the corresponding RGF reconstruction is shown in Fig. 5.3(b).

In the fourth experiment, the more realistic phantom of Fig. 5.4(a) is considered. Here the electrical parameters of the healthy fat are perturbed with components randomly drawn from a uniform distribution within 10% around the unperturbed values; moreover, six veins and one gland are placed into the breast. Two veins are in the imaging plane, while the other four flow in the orthogonal direction; the gland is just along one of the two veins (the vertical one, on the right) in the imaging plane. Of course, this perturbation is not coded into the Green's function, which then remains the same as in the previous cases. Finally, a circular tumor with a diameter of $1.50 \cdot 10^{-2}$ m is placed into this phantom. The application of the visualization algorithm leads to the reconstruction of Fig. 5.4(b), where the tumor is clearly visible, although the limited resolution of the procedure is pointed out by an increase of its diameter, as shown by a comparison with the visualization of Fig. 5.1(b).

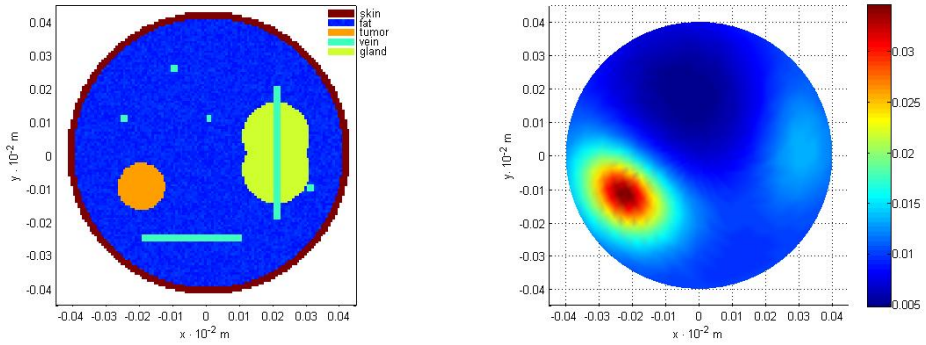

FIG. 5.4. *(a) Phantom of the breast: the healthy fat is perturbed with components randomly drawn from a uniform distribution within* 10% *around the unperturbed values; moreover, six veins and one gland are added inside the fat tissue. A circular tumor, centred in* $(-2.00, -1.00) \cdot 10^{-2}$ m *and with a diameter of* $1.50 \cdot 10^{-2}$ m *is also placed in the breast. (b) Visualization provided by the RGF algorithm.*

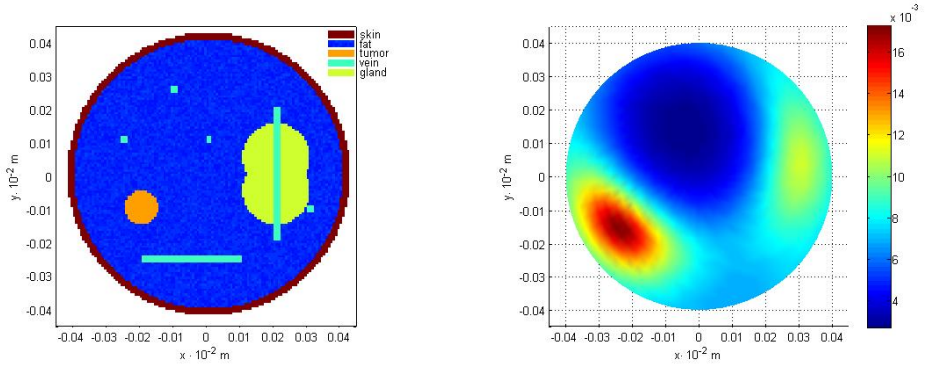

FIG. 5.5. *(a) Phantom of the breast: the healthy fat is perturbed with components randomly drawn from a uniform distribution within* 10% *around the unperturbed values; moreover, six veins and one gland are added inside the fat tissue. A circular tumor, centred in* $(-2.00, -1.00) \cdot 10^{-2}$ m *and with a diameter of* $1.00 \cdot 10^{-2}$ m *is also placed in the breast. (b) Visualization provided by the RGF algorithm.*

As one could expect, the perturbation of the healthy background becomes increasingly important as the size of the tumor diminishes. This effect is highlighted by the fifth simulation, in which a circular tumor with a diameter of $1.00 \cdot 10^{-2}$ m is placed into the same perturbed background as before: the phantom is shown in Fig. 5.5(a). In the visualization provided by the RGF algorithm and represented in Fig. 5.5(b), the tumor is still detectable, but, mainly due to the veins in the imaging plane, its size tends to be overestimated and an artefact appears on the right. Therefore, under these conditions, the distinction between the tumor and the artefact can be obtained by means of a different imaging modality providing some quantitative information on the different kinds of tissue.

Although, a priori, the RGF method can visualize a tumor only if $G(\cdot, y)$ is exactly known, the previous simulations show that reliable reconstructions can be obtained even with a non complete knowledge of $G(\cdot, y)$, i.e. when only the Green's function

corresponding to fat, skin and free space is available.

6. Conclusions and future developments. In this paper we generalize the formulation and improve the implementation of a linear qualitative method, based on the so-called "reciprocity gap functional", for solving inverse scattering problems that are, in general, genuinely non-linear, i.e. allow no realistic linearizing approximation. Furthermore, we apply this approach for the first time to the visualization of breast cancer in a microwave tomography setting. From the theoretical viewpoint, the generalization consists in developing a formulation that takes into account the possible heterogeneity of the background medium inside the array of receiving antennas: in particular, if this background is lossy, an interior transmission problem with complex wavenumbers needs to be discussed, in order to show that transmission eigenvalues form a discrete set. Although our focus is on the inverse problem of microwave tomography for breast cancer detection, other scattering situations (for penetrable targets) are easily incorporated in our framework by considering the proper Green's function; moreover, an analogous generalization could also be carried out in the case of impenetrable scatterers. From the viewpoint of implementation, the improvement consists in adopting a "no-sampling" approach, which provides very fast 2D reconstructions of the breast: indeed, the computational times of the RGF algorithm are around 1 s.

The real impact of this imaging technique should be evaluated by comparing it with other existing inversion methods, both qualitative (such as the linear sampling method for near-field measurements [8]) and quantitative (such as the CGLS algorithm proposed in [23]): to this aim, it would be interesting to perform a theoretical and operative analysis of the RGF method in order to assess the resolution achievable and to estimate the optimal number of antennas surrounding the breast, i.e. the minimum number of measurements collecting all the retrievable information.

Of course, a weak point of the RGF algorithm is that the physical and geometrical properties of the healthy breast should be known a priori. This prior knowledge could be available, at least approximately, from previous clinical exams (e.g. MRI) of the same patient. In any case, future research should be devoted to assessing the stability and reliability of the RGF method with respect to uncertainties in the Green's function describing the healthy breast: in this context, our first results, as shown in Fig. 5.4 and Fig. 5.5, seem to highlight a promising robustness of the RGF algorithm.

M. B. has been supported by a grant of the Italian Istituto Nazionale di Alta Matematica (INdAM).

Appendix A. General theorems. In this appendix, our purpose is to briefly prove two theorems used in the paper.

The first theorem is the generalization for k not constant of Theorem 2.12 in [13].

THEOREM A.1. *Let W be an open bounded Lipschitz domain such that $\mathbb{R}^2 \setminus \overline{W}$ is connected; let $k \in L^\infty(\mathbb{R}^2 \setminus \overline{W})$ and $R > 0$ such that $k(x) = k_0 \in \mathbb{R}^*_+ = (0, +\infty)$ for $|x| \geq R$. Moreover, let u be the unique solution of the following problem:*

$$\begin{cases} \Delta u + k^2(x)u = 0 \quad \text{in} \quad \mathbb{R}^2 \setminus \overline{W} \\ u = 0 \quad \text{on} \quad \partial W \\ \lim\limits_{r\to\infty} \sqrt{r}(\partial_r u - \mathrm{i}k_0 u) = 0. \end{cases} \tag{A.1}$$

Then, it holds $u = 0$ in $\mathbb{R}^2 \setminus \overline{W}$.

Proof. Let $r \geq R$ be such that the open ball B_r with centre in the origin O and radius r contains $\overline{W}$. If we put $S_r := \partial B_r$ and we remember the first two equations in (A.1), as well as the hypothesis $k(x) = k_0$ for $|x| \geq R$, then the

first Green's identity [20] shows that $\int_{S_r} u(x)\partial_\nu \overline{u}(x)\, ds(x) = \int_{B_r\setminus\overline{W}} |\nabla u(x)|^2\, dx - \int_{B_r\setminus\overline{W}} k_0^2 |u(x)|^2\, dx$. Taking the imaginary part of each term in this equation, we get $\Im m\left\{\int_{S_r} u(x)\partial_\nu \overline{u}(x)\, ds(x)\right\} = 0$. Hence, by virtue of Theorem 2.12 in [13], we deduce that $u = 0$ in $\mathbb{R}^2 \setminus \overline{B}_r$ and then the unique continuation principle ensures that $u = 0$ in $\mathbb{R}^2 \setminus \overline{W}$. □

The second theorem links the injectivity of the single layer operator on the boundary of a domain to the solvability of the Dirichlet problem.

THEOREM A.2. *Let W be a bounded Lipschitz domain and let $W' \subset W$ be an open subset of W; if $k \in L^\infty(W)$ is such that $\Im m\left\{k^2(x)\right\} \geq 0$ f.a.a. $x \in W$ and $\Im m\left\{k^2(x)\right\} \geq c > 0$ f.a.a. $x \in W'$, then the single layer operator $S_{\partial W} : H^{-\frac{1}{2}}(\partial W) \to H^{\frac{1}{2}}(\partial W)$ is bijective.*

Proof. Let $\varphi \in H^{-\frac{1}{2}}(\partial W)$ be such that $S_{\partial W}\varphi = 0$ and let v be the single layer potential of density φ, i.e. $v(x) := \int_{\partial W} G(x,y)\varphi(y)\, ds(y)\ \forall x \in \mathbb{R}^2 \setminus \partial W$. Then, in particular, v solves the following Dirichlet problem: $\Delta v + k^2(x)v = 0$ in W and $v = 0$ on ∂W. Hence, by using the first Green's identity in W, we get $-\int_W |\nabla v(x)|^2\, dx + \int_W k^2(x)|v(x)|^2\, dx = 0$ and, by taking the imaginary part of each term in this equation, we have $\int_W \Im m\left\{k^2(x)\right\} |v(x)|^2\, dx = 0$. By virtue of the hypotheses made on $\Im m\left\{k^2(x)\right\}$, we find $\int_{W'} |v(x)|^2\, dx = 0$: hence $v = 0$ in W' and by the unique continuation principle $v = 0$ in W. Then, in particular, $\partial_\nu v^- = 0$. Moreover v is a solution of problem (A.1) and Theorem A.1 ensures that $v = 0$ in $\mathbb{R}^2 \setminus \overline{W}$: then $\partial_\nu v^+ = 0$. Now, according to the jump relations [20] for the single layer potentials, it holds $-\varphi = \partial_\nu v^+ - \partial_\nu v^-$: hence $\varphi = 0$ and this shows the injectivity of $S_{\partial W}$. Since $S_{\partial W}$ is a Fredholm operator of index 0 [20], it is also bijective. □

Appendix B. The interior transmission problem. Let D be an open bounded Lipschitz domain and let us consider the following interior transmission problem: for all $h \in H^1_\Delta(D)$, find $u, v \in H^0_\Delta(D)$ such that $u - v \in H^1_\Delta(D)$ and

$$\begin{cases} \Delta u + k^2 n_1(k) u = 0 & \text{in } D \\ \Delta v + k^2 n_D(k)(x) v = 0 & \text{in } D \\ (u - v) = h & \text{on } \partial D \\ \partial_\nu (u - v) = \partial_\nu h & \text{on } \partial D, \end{cases} \tag{B.1}$$

where $k \in \mathbb{R}^*_+ = (0, +\infty)$, $n_1 : \mathbb{R}^*_+ \to \mathbb{C}$ is a complex-valued function of the real variable k and $n_D : \mathbb{R}^*_+ \to L^\infty(D)$ is a function of the real variable k with values in the space $L^\infty(D)$. We now want to show that under some assumptions the problem (B.1) has a unique solution.

We firstly consider the homogeneous version of problem (B.1), i.e. the case in which the function h is identically zero, and we want to show that this problem has only the trivial solution, except for a discrete set of values for k. Then, if we call "set of transmission eigenvalues" the set of values of k such that the homogeneous transmission problem has a non trivial solution, this means that the set of transmission eigenvalues is a discrete subset of $\mathbb{R}^*_+$.

Following the same steps as in [24], the following lemma for the homogeneous interior transmission problem can be easily proved.

LEMMA B.1. *Put $m(k) := n_1(k) - n_D(k)$ for all $k \in (0, \infty)$, if k is such that $m^{-1}(k) \in L^\infty(D)$, then the homogeneous transmission problem has a non trivial solution if and only if there exists a nontrivial function $w \in H^1_{\Delta,0}(D)$ such that $F_k(w, \psi) = 0\ \forall \psi \in H^1_{\Delta,0}(D)$, where $H^1_{\Delta,0}(D)$ is the Hilbert space defined as $H^1_{\Delta,0}(D) := \{u \in$*

$H^1_\Delta(D) : u = \partial_\nu u = 0 \text{ on } \partial D\}$, *and* F_k *is the bounded sesquilinear form defined on* $H^1_{\Delta,0}(D)$ *as*

$$F_k(\phi,\psi) := \int_D m^{-1}(k)(x)\left[\Delta + k^2 n_1(k)\right]\phi(x)\ \left[\Delta + k^2 n_D(k)\right]\overline{\psi}(x)\,dx = \qquad \text{(B.2)}$$
$$= \left(m^{-1}(k)\left[\Delta + k^2 n_1(k)\right]\phi, \left[\Delta + k^2 \overline{n}_D(k)\right]\psi\right)_0 \quad \forall \phi,\psi \in H^1_{\Delta,0}(D),$$

having denoted with $(\cdot,\cdot)_0$ *the scalar product in* $L^2(D)$.

Now, for all $k \in \mathbb{R}^*_+$ such that $m^{-1}(k) \in L^\infty(D)$, let us define the following sesquilinear forms: $\forall \phi,\psi \in H^1_{\Delta,0}(D)$,

$$F^0_k(\phi,\psi) := (m^{-1}(k)\Delta\phi, \Delta\psi)_0, \quad F^1_k(\phi,\psi) := k^2(m^{-1}(k)n_1(k)\phi, \Delta\psi)_0, \qquad \text{(B.3)}$$
$$F^D_k(\phi,\psi) := k^2(m^{-1}(k)\Delta\phi, \overline{n}_D(k)\psi)_0, \quad F^{1D}_k(\phi,\psi) := k^4(m^{-1}(k)n_1(k)\phi, \overline{n}_D(k)\psi)_0.$$

Then, it is obvious that for all $k \in \mathbb{R}^*_+$ such that $m^{-1}(k) \in L^\infty(D)$ it holds $F_k = F^0_k + F^1_k + F^D_k + F^{1D}_k$. Moreover, it can be easily shown that the following sesquilinear form on $H^1_{\Delta,0}(D)$

$$\forall u, v \in H^1_{\Delta,0}(D), \quad (u,v)_{\Delta,0} := (\Delta u, \Delta v)_0 \qquad \text{(B.4)}$$

defines a scalar product on $H^1_{\Delta,0}(D)$ equivalent to the H^1_Δ scalar product. Then, according to the Lax-Milgram theorem, for all $k \in \mathbb{R}^*_+$ such that $m^{-1}(k) \in L^\infty(D)$ we can introduce the operators associated to the previous forms (B.2), (B.3), i.e. the operators in $H^1_{\Delta,0}(D)$ defined as

$$(S_k\phi,\psi)_{\Delta,0} := F_k(\phi,\psi), \quad (S^0_k\phi,\psi)_{\Delta,0} := F^0_k(\phi,\psi), \quad (S^1_k\phi,\psi)_{\Delta,0} := F^1_k(\phi,\psi),$$
$$(S^D_k\phi,\psi)_{\Delta,0} := F^D_k(\phi,\psi), \quad (S^{1D}_k\phi,\psi)_{\Delta,0} := F^{1D}_k(\phi,\psi) \quad \forall \phi,\psi \in H^1_{\Delta,0}(D). \qquad \text{(B.5)}$$

Then we have $S_k = S^0_k + S^1_k + S^D_k + S^{1D}_k$. We now make the following assumptions:

1) n_1 and n_D are analytic functions of k on $\mathbb{R}^*_+$: in this case we know that there exists an open connected set $W \subset \mathbb{C}$ containing $\mathbb{R}^*_+$ such that n_1 and n_D can be continued to analytic functions in W and for all such sets W the continuation is unique;
2) among the previous sets W, there exists a set $\tilde{W}$ such that the set $Sing(m) := \{z \in \tilde{W} : m^{-1}(z) \notin L^\infty(D)\}$ is discrete;
3) there exists an open connected subset X of $\tilde{W} \setminus Sing(m)$ containing $\mathbb{R}^*_+ \setminus Sing(m)$ such that, for all $z \in X$, either $\Re e\left\{m^{-1}(z)\right\} > c_z > 0$ on D, or $\Im m\left\{m^{-1}(z)\right\} > c_z > 0$ on D, or $\Re e\left\{m^{-1}(z)\right\} < -c_z < 0$ on D, or $\Im m\left\{m^{-1}(z)\right\} < -c_z < 0$ on D, where, for all $z \in X$, c_z is a positive constant, depending on z and verifying $\left\|m^{-1}(z)\right\|_\infty = o\left(\frac{c_z}{z^2}\right)$ as $z \to 0$;
4) n_1 and n_D are bounded when $k \in \mathbb{R}^*_+$ goes to 0.

Remark B.1. In the case of $n_D(k)$ independent of x, assumption 1) implies assumptions 2) and 3). Therefore, in this case, only assumptions 1) and 4) need a physical justification, which is given by the Havriliak-Negami model for dielectric relaxation [14].

As in [24], by exploiting the previous decomposition $S_k = S^0_k + S^1_k + S^D_k + S^{1D}_k$, we can prove that S_k is a Fredholm operator of index 0. Then, by using the analytic Fredholm theory, we can show that S_k is non-singular except for a discrete set of values of k: this task is accomplished by the following three theorems.

THEOREM B.2. *Let $z \in X$: then the operators S_z^1, S_z^D and S_z^{1D} are compact.*

Proof. For all $\phi \in H^1_{\Delta,0}(D)$, from definitions (B.3), (B.4) and (B.5) we have:

$$\begin{aligned}
\left(\Delta S_z^1\phi, \Delta S_z^1\phi\right)_0 &= (S_z^1\phi, S_z^1\phi)_{\Delta,0} = F_z^1(\phi, S_z^1\phi) = z^2\left(m^{-1}(z)n_1(z)\phi, \Delta S_z^1\phi\right)_0, \\
\left(\Delta S_z^D\phi, \Delta S_z^D\phi\right)_0 &= \left(S_z^D\phi, S_z^D\phi\right)_{\Delta,0} = F_z^D(\phi, S_z^D\phi) = z^2\left(m^{-1}(z)\Delta\phi, \overline{n}_D(z)S_z^D\phi\right)_0, \\
\left(\Delta S_z^{1D}\phi, \Delta S_z^{1D}\phi\right)_0 &= \left(S_z^{1D}\phi, S_z^{1D}\phi\right)_{\Delta,0} = F_z^{1D}(\phi, S_z^{1D}\phi) = \\
&= z^4\left(m^{-1}(z)n_1(z)\phi, \overline{n}_D(z)S_z^{1D}\phi\right)_0,
\end{aligned}$$

whence we respectively get, for all $\phi \in H^1_{\Delta,0}(D)$,

$$\|S_z^1\phi\|_{\Delta,0} \leq |z|^2 \|m^{-1}(z)\|_\infty |n_1(z)| \|\phi\|_0, \tag{B.6}$$

$$\|S_z^D\phi\|^2_{\Delta,0} \leq |z|^2 \|m^{-1}(z)\|_\infty \|n_D(z)\|_\infty \|\phi\|_{\Delta,0} \|S_z^D\phi\|_0, \tag{B.7}$$

$$\|S_z^{1D}\phi\|^2_{\Delta,0} \leq |z|^4 \|m^{-1}(z)\|_\infty \|n_D(z)\|_\infty |n_1(z)| \|\phi\|_0 \|S_z^{1D}\phi\|_0. \tag{B.8}$$

Since the injection $H^1_{\Delta,0}(D) \hookrightarrow L^2(D)$ is compact, inequalities (B.6), (B.7) and (B.8) prove the compactness of S_z^1, S_z^D and S_z^{1D} respectively. □

THEOREM B.3. *For all $z \in X$, the operator S_z^0 is non-singular.*

Proof. For all $\phi \in H^1_{\Delta,0}(D)$, by virtue of definitions (B.3) and (B.5) we have $(S_z^0\phi, \phi)_{\Delta,0} = F_z^0(\phi, \phi) = (m^{-1}(z)\Delta\phi, \Delta\phi)_0$. Hence, by using the previous assumption No. 3 on $m^{-1}(z)$, we can deduce that either $\pm S_k^0$ or $\pm \mathrm{i} S_k^0$ is positive and bounded below, and then S_k^0 is non-singular. □

THEOREM B.4. *The operator S_k is non-singular except for a discrete set of values of $k \in \mathbb{R}_+^*$.*

Proof. Let $\eta \in \mathbb{R}_+^*$ such that $\|\phi\|_0 \leq \eta\|\phi\|_{\Delta,0}$ for all $\phi \in H^1_{\Delta,0}(D)$. According to assumptions 3 and 4, we can consider $k \in (0,1) \setminus Sing(m)$ such that

$$\begin{aligned}
|n_1(k)| \left\|m^{-1}(k)\right\|_\infty &\leq \frac{c_k}{4\eta}, \\
\|n_D(k)\|_\infty \left\|m^{-1}(k)\right\|_\infty &\leq \frac{c_k}{4\eta}, \\
|n_1(k)| \|n_D(k)\|_\infty \left\|m^{-1}(k)\right\|_\infty &\leq \frac{c_k}{4\eta^2}.
\end{aligned} \tag{B.9}$$

Without loss of generality, replacing S_k by $-S_k$ or $\pm \mathrm{i} S_k$ if needed, we can suppose that $\Re e\left(m^{-1}(k)\right) > c_k > 0$. Then, by using inequalities (B.6), (B.7), (B.8) and (B.9), for all $\phi \in H^1_{\Delta,0}(D)$, we get $\Re\left((S_k\phi, \phi)_{\Delta,0}\right) \geq \frac{c_k}{4}\|\phi\|_{\Delta,0}$. Thus S_k is positive and bounded below and then invertible. Hence, by using the analytic Riesz-Fredholm theory, it turns out that S_z is non-singular except for a discrete subset of X: as a consequence, S_k is non-singular except for a discrete set of values of $k \in \mathbb{R}_+^*$. □

COROLLARY B.5. *The set of transmission eigenvalues is a discrete subset of $\mathbb{R}_+^*$.*

Proof. It follows from Lemma B.1 that the set of transmission eigenvalues in $k \in \mathbb{R}_+^* \setminus Sing(m)$ is the set of k such that S_k is non injective. Now, by Theorem B.2 and Theorem B.3, S_k is a Fredholm operator of index 0 for all $k \in \mathbb{R}_+^* \setminus Sing(m)$, so that $k \in \mathbb{R}_+^* \setminus Sing(m)$ is a transmission eigenvalue if and only if S_k is singular, but by Theorem B.4 this holds only for a discrete set. Finally, since we supposed that the set $Sing(m)$ is discrete, the transmission eigenvalues form a discrete subset of $\mathbb{R}_+^*$. □

We can now state the main and last theorem of this section, which can be proved analogously to Theorem 4.1 in [24].

THEOREM B.6. *If $k \in \mathbb{R}_+^* \setminus Sing(m)$ is not a transmission eigenvalue, then for all $h \in H^1_\Delta(D)$ the inhomogeneous transmission problem (B.1) has a unique solution.*

REFERENCES

[1] R. A. Albanese, R. L. Medina and J. W. Penn, *Mathematics, medicine and microwaves*, Inverse Problems, 10 (1994), pp. 995-1007.

[2] R. Aramini, *On Some Open Problems in the Implementation of the Linear Sampling Method*, Ph.D. thesis, Dipartimento di Matematica, Università di Trento, 2007.

[3] R. Aramini, M. Brignone and M. Piana, *The linear sampling method without sampling*, Inverse Problems, 22 (2006), pp. 2237-2254.

[4] M. Bertero, *Linear inverse and ill-posed problems* in Advances in Electronics and Electron Physics, Hawkes P. W. (ed), 1989, Academic, New York.

[5] M. Brignone, G. Bozza, R. Aramini, M. Pastorino and M. Piana, *A fully no-sampling formulation of the linear sampling method for three-dimensional inverse electromagnetic scattering problems*, Inverse Problems, 25 (2009), 015014.

[6] A. E. Bulyshev, S. Y. Semenov, A. E. Souvorov, R. H. Svenson, A. G. Nazarov, Y. E. Sizov and G. P. Tatsis, *Computational modeling of three-dimensional microwave tomography of breast cancer*, IEEE Trans. Biomed. Eng. 48 (2001), pp. 1053-1056.

[7] F. Cakoni and D. Colton, *Qualitative Methods in Inverse Scattering Theory*, Springer, Berlin, 2006.

[8] F. Cakoni, M. Fares and H. Haddar, *Analysis of two linear sampling methods applied to electromagnetic imaging of buried objects*, Inverse Problems, 22 (2006), pp. 845-867.

[9] D. Colton and H. Haddar, *An application of the reciprocity gap functional to inverse scattering theory*, Inverse Problems, 21 (2005), pp. 383-398.

[10] D. Colton and P. Monk, *A linear sampling method for the detection of leukemia using microwaves*, SIAM J. Applied Math., 58 (1998), pp. 926-941.

[11] D. Colton and P. Monk, *A linear sampling method for the detection of leukemia using microwaves II*, SIAM J. Applied Math., 60 (1999), pp. 241-255.

[12] D. Colton, M. Piana and R. Potthast, *A simple method using Morozov's discrepancy principle for solving inverse scattering problems*, Inverse Problems, 13 (1997), pp. 1477-1493.

[13] D. Colton and R. Kress, *Inverse Acoustic and Electromagnetic Scattering Theory*, 2nd edition, Springer, Berlin, 1998.

[14] D. K. Das-Gupta and P. C. N. Scarpa, *Modeling of Dielectric Relaxation Spectra of Polymers in the Condensed Phase*, IEEE El. Insul. Mag., 15 (1999), pp. 23-37.

[15] J. Devaney, *Diffraction tomography in Inverse Methods in Electromagnetic Imaging*, W. M. Boerner et al. (Eds.), 1985, D. Reidel Publishing, Boston.

[16] H. W. Engl, M. Hanke and A. Neubauer, *Regularization of Inverse Problems*, Kluwer Academic Publishers, Dordrecht, 1996.

[17] S. C. Hagness, A. Taflove and J. E. Bridges, *Two-Dimensional FDTD Analysis of a Pulsed Microwave Confocal System for Breast Cancer Detection: Fixed-Focus and Antenna-Array Sensors*, IEEE Trans. Biomed. Eng., 45 (1998), pp. 1470-1479.

[18] L. D. Landau and E. M. Lifshitz, *Electrodynamics of continuous media*, vol. 8 of the *Course of Theoretical Physics*, 2nd edition, Pergamon Press, 1984.

[19] R. Leis, *Initial Boundary Value Problems in Mathematical Physics*, John Wiley, New York, 1986.

[20] W. McLean, *Strongly Elliptic Systems and Boundary Integral Equations*, Cambridge University Press, New York, 2000.

[21] P. Monk, *Finite Element Methods for Maxwell's Equations*, Oxford University Press, New York, 2003.

[22] J. H. Richmond, *Scattering by a dielectric cylinder of arbitrary cross section shape*, IEEE Trans. Ant. Prop., 13 (1965), pp. 334-341.

[23] T. Rubaek, P. M. Meaney, P. Meincke and K. D. Paulsen, *Nonlinear Microwave Imaging for Breast-Cancer Screening Using Gauss-Newton's Method and the CGLS Inversion Algorithm*, IEEE Trans. Ant. Prop., 55 (2007), pp. 2320-2331.

[24] B. P. Rynne and B. D. Sleeman, *The interior transmission problem and inverse scattering from inhomogeneous media*, SIAM J. Math. Anal., 22 (1991), pp. 1755-1762.

[25] A. N. Tikhonov, A. V. Goncharsky, V. V. Stepanov and A. G. Yagola, *Numerical Methods for the Solution of Ill-Posed Problems*, Kluwer Academic Publishers, Dordrecht, 1996.